When the ebbing tide retreats along the rocky shoreline
It leaves a trail of tidal pools
Each microcosmic planet
A complete society….
All the busy little creatures chasing out their destinies
Living in their pools
They soon forget about the sea....

Neil Peart

University of Alberta

Burrow associated reservoir quality in marine siliciclastic sediments.

By

John Borthwick Gordon

A thesis submitted to the Faculty of Graduate Studies and Research in partial fulfillment of the requirements for the degree of Master of Science

Department of Earth and Atmospheric Sciences

Spring, 2010
Edmonton, Alberta

Examining Committee

Dr. George Pemberton; Earth and Atmospheric Science

Dr. Murray K. Gingras; Earth and Atmospheric Science

Dr. David K Potter, Earth and Atmospheric Science

This thesis is dedicated to my children.
See, you can teach an old dog new tricks.

Abstract

Burrow-associated diagenetic alteration and eventual reservoir quality parameters such as porosity and permeability may be altered due to reorganization of the sediment fabric associated with animal burrowing, or result from heterogeneous cement distribution influenced by the bioturbate texture.

Petrographic analysis has significant application in recognizing burrow-associated porosity characteristics in marine sandstones. Petrographic analysis can provide mineral identification due to diagenetic chemical alterations and textural evidence regarding cementation history that can lead to more accurate hydrocarbon target interpretations.

Overlooking burrow structures may lead to misinterpretations of permeability streaks in hydrocarbon reservoirs. This may be extremely important for reservoirs where slight permeability variations have an effect on hydrocarbon reserve calculations.

Understanding biogeochemical reactions and burrow-associated diagenesis that ultimately control reservoir quality is necessary if production from ancient bioturbated marine sandstone reservoirs is to be optimized.

Acknowledgments

I would like to thank Dr. Murray Gingras, Dr. George Pemberton, and Dr. Kurt Konhauser for their insights and suggestions that greatly improved the quality of this thesis.

I am greatly indebted to Dr. Richard Evoy at Suncor Energy Inc. (formerly Petro Canada Oil and Gas) for his many suggestions, comments, and recommendations that really helped me to focus and complete this thesis. All those geological concepts on Starbuck's napkins really helped. I also thank Dr. Evoy and Suncor Energy Inc (formerly Petro Canada Oil and Gas) for permitting me access to all of the petrographic equipment and thin-section database.

This thesis greatly benefited from the expert reviews of Dr. David Potter and Dr. John-Paul Zonneveld at the University of Alberta.

I especially would like to thank my wife Tammy for being supportive through this whole process. It is not an easy feat to write a thesis at 45 years old and I could not have done it without her patience.

I thank Jason Lavigne at Talisman Energy who graciously donated the use of the 100/06-24-076-07W6/00 slabbed core. Jussi Hovikoski at the University of Alberta is thanked for offering his time for instruction on the minipermeameter and core handling.

Lastly I thank the Natural Sciences and Engineering Research Council Operating Grants to M. K. Gingras, S. G. Pemberton, K. Konhauser and an equipment grant to M. K. Gingras. The Alberta Science Research Authority is also thanked for a generous equipment grant made to K. Konhauser and S. G. Pemberton.

Table of Contents

List of Tables

List of Figures

Chapter 1: Introduction

1.1 Opening Statement and Objectives

Diagenesis can be defined as any chemical, physical, or biological change undergone by a sediment after its initial deposition. These changes can include compaction; mineral transformation; organic matter degradation; generation of hydrocarbons; change in pore water composition; bioturbation; and the cementation of unconsolidated sediment (Konhauser, 2007). Diagenesis of siliciclastic sandstones begins immediately upon deposition in marine sediments. At or near the sediment-water interface the porosity of the sediment is at a maximum. Within only a few centimetres of burial the diagenetic process begins by compaction of the sediment and compartmentalizing pore fluids. Upon further burial of the sediment porosity loss becomes greater, pore fluids are reduced, and lithification of the sediment begins. Choquette and Pray (1970) provide a three-fold classification scheme for time and depth related diagenesis intended for carbonate rocks, but also applies to siliciclastic diagenesis: 1) Eogenetic (occurring very early at low temperature and in proximity to the surface; 2) Mesogenetic (occurring during burial, but still closely related to surface processes; and 3) Telogenetic (occurring after sediment burial and after significant uplift due to tectonics and/or diagenetic reactions association with unconformities).

Marine environments can support a large population of burrowing macrofauna invertebrates, which have a significant effect on solute

exchange and early diagenetic processes at the sediment-water interface (Kristensen, 2001). Recently several authors (Zhu et al., 2006; Zorn et al., 2006; Pemberton and Gingras, 2005; McIlroy et al., 2003; Gingras et al., 2002; and Aller, 1994) have shown that the burrowing activities of marine invertebrates such as reworking of sediment, irrigation, and excretion result in extreme biogeochemical heterogeneities within the sediment. As important, burrows may provide nucleation sites for the precipitation of early diagenetic cements.

Marine environments receive organic carbon inputs derived from both terrestrial and marine sources (Hedges and Parker, 1976). Organic matter consists of complex compounds; aquatic organisms contribute proteins, lipids, and carbohydrates while plants contribute resins, waxes, lignin and carbohydrates in the form of cellulose (Barnes et al, 1990). In a sedimentary sequence an idealized biogeochemical zonation exists based on the burial and subsequent degradation of organic carbon. This predictable succession of microbial metabolism of organic matter is aerobic respiration followed by anaerobic respiration including denitrification; reduction of manganese; reduction of iron; sulphate reduction; and methanogenesis (Konhauser, 2007). The interaction of these vertical biogeochemical zones can become extremely disrupted in the presence of burrowing fauna that may facilitate a cascade of redox reactions affecting the diagenesis of a particular sediment. Figure 1.1 shows an idealized representation of these biogeochemical zones. A

partial range of burrow types and how they react with the biogeochemical zones is also shown.

Of particular interest amongst marine depositional environments are shoreface deposits. Prothero and Schwab (1996) show a typical shoreface as a coarsening upward sequence of mature quartz, rare feldspar, and chert-rich sand of fine to medium grain size with multidirectional trough cross beds interbedded with low-dipping tabular and planar cross beds being positioned in high-energy surf zones and lie landward of the breaker zone in nearshore environments. Trace fossils are of low diversity, but can be locally abundant. Ancient shoreface deposits are of economical significance because they are often associated with large accumulations of hydrocarbons, can have great lateral extent, be predictable, and are mappable in the subsurface.

A multidisciplinary approach is required to understand the influence of ichnological activity and how porosity and permeability are affected by burrow-associated diagenetic alterations in shoreface sandstones. Pemberton and Gingras (2005) have shown that overlooking burrow-associated diagenesis can lead to inaccurate assessments of the flow characteristics or non-recognition of permeability streaks in hydrocarbon reservoirs. This may be extremely important as North American hydrocarbon exploitation companies move away from depleting conventional style oil and gas plays. Increasing interest from these companies is leaning towards producing hydrocarbons from shallow, low-

rate, low permeability, thinly laminated, muddy, bioturbated units that are thick, laterally extensive, and most importantly are interbedded with source rock. These play types need to be artificially stimulated to produce hydrocarbons.

The objective of this thesis is to show how detailed petrographic examination of micro-fabrics with is essential to assessing reservoir quality using examples from ancient shoreface sandstone where it is evident that burrow-associated diagenesis has enhanced or degraded reservoir quality. Petrographic analysis presents informative views of mineralogical controls affecting reservoir quality, but is commonly overlooked due to the reliance on wireline log analysis and other large-scale reservoir evaluation tools such as numerical engineering models. Petrography potentially provides a window into small-scale burrow-associated heterogeneities and the geochemical evolution of early diagenetic reactions that occur during the subsequent burial of the sediment. Authigenic mineral phases can be readily identified as well as fabric and textural characteristics such as grain-size, grain-packing, and grain-shape with common petrographic tools such as thin section analysis, x-ray diffraction (XRD), and scanning electron microscopy (SEM). This type of data is inexpensively acquired and can lead to reasonable diagenetic history interpretations that influence the outcome of hydrocarbon reservoir evaluation.

1.2 Thesis Outline

Chapter 1 is an introduction focusing on an opening statement, the utility of petrographic technique, and objectives of the thesis.

Chapter 2 presents the utility of simple petrographic observations using twenty-five samples collected from five different formations from Alaska, central Alberta, and offshore Newfoundland. These samples represent various burrow-associated porosity characteristic and chemical eogenetic alterations ranging from complete cementation of burrows with carbonate cement, silica cement, and early authigenic clay to complete dissolution of cement inside burrow leading to excellent local preservation of reservoir quality.

These examples were chosen because they have been significant targets for oil and gas companies and they provide excellent examples of porosity heterogeneity caused by burrow-associated early diagenesis. These examples are in no way a complete categorization of burrow-associated diagenesis and do not show complete formation or reservoir evaluation of the areas chosen, but do show that burrow-associated reservoir quality is wide spread and is common in the rock record and should not be ignored.

Chapter 3 presents a core study completed on the Cretaceous-aged Bluesky Formation from the LaGlace area of Alberta. The Bluesky Formation in the La Glace area represents a high-energy, upper shoreface

succession that provides an excellent case study for the utility of petrographic analysis pertaining to biogenically enhanced reservoir quality because (1) the Bluesky Formation is a significant gas-bearing reservoir in the area; (2) there is locally good core control; and (3) burrow-associated enhanced permeability is evident. Several cores were described, but only one core is illustrated to show the reservoir rock is an upper fine to lower-medium grained chert-rich litharenite that is intensely bioturbated with *Macaronichnus segregatus*. High measured permeability corresponds to this bioturbated zone. Utilization of thin sections and scanning electron microscopy has led to the interpretation that the tracemaker of *Macaronichnus segregatus* avoided iron-rich detrital fragments while exploiting the sediment for food. This grain avoidance led to a re-sorting of the sand that shed the dark-coloured rock fragments to outline the burrow while light-coloured competent grains were ingested and became the burrow fill. The light-coloured burrow fill contains a high chert to quartz ratio. Primary reservoir quality can be preserved in the presence of chert as pore-occluding quartz overgrowths do no form on chert fragments as they do on monocrystalline quartz, thus leaving open, well connected primary pores and hence elevated permeability.

Chapter 4 is the conclusion of the previous chapters discussing the significance of recognizing burrow-associated diagenetic fabric as they apply to preserved and/or destroyed reservoir quality.

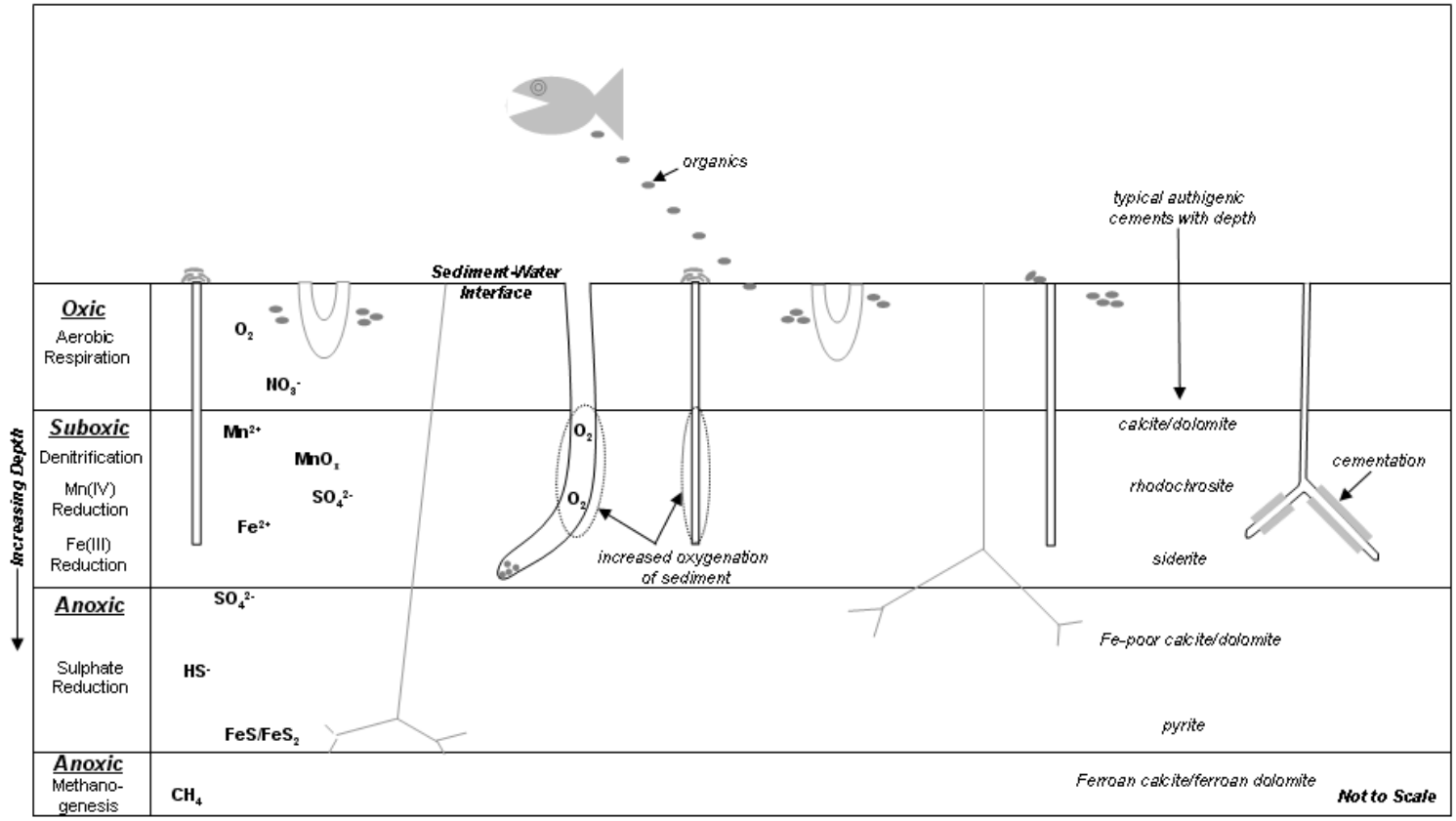

Figure 1.1 Biogeochemical zones of organic-inorganic interactions with burial depth of organic matter and marine siliciclastic sediment. A partial range of burrow types have been added to show how they react within the oxic, suboxic, and anoxic zones. Note how burrows can act as extensions of the sediment-water interface allowing oxygen and other nutrients to penetrate previously depleted zones. Typical authigenic carbonate cements that can precipitate in these zones are shown. The actual thickness of each zone is largely dependant on sedimentation rate (modified from Konhauser and Gingras, 2007; Morad, 1998; Berner, 1991; and Hesse, 1990).

1.3 References

Aller, R.C., 1994, Bioturbation and remineralization of sedimentary organic matter: effects of redox oscillation: Chemical Geology 114, p. 331- 345.

Choquette, P. W., and L. C. Pray, 1970, Geologic nomenclature and classification of porosity in sedimentary carbonates: AAPG Bulletin., v. 54, p. 207-250.

Gingras, M.K., B. MacMillan, B. J. Balcom, T. Saunders, S. G. Pemberton, 2002, Using resonance imaging and petrographic techniques to understand the textural attributes and porosity distribution in Macaronichnus-burrowed sandstone: Journal of Sedimentary Research, v. 72, No. 4, p 552-558.

Hedges, J.I., P. L. Parker, 1976, Land derived organic matter in the surface sediment from the Gulf of Mexico: Geochimica et Cosmochemica Acta 40, p. 1019-1029.

Konhauser, K.O. 2007. Introduction to Geomicrobiology: Blackwell Publishing USA.

Kristensen, E., 2001, Impact of polychaetes (Nereis spp. and Arenicola marina) on carbon biogeochemistry in coastal marine sediments: Geochemical Transcripts. v.12, p 1-11.

McIlroy, D., R. H. Worden, S. J. Needham, 2003, Faeces, clay mineral and reservoir potential: Journal of the Geological Society, London, v. 160, p. 489-493.

Pemberton, S.G., M. K. Gingras, 2005, Classification and characterizations of biogenically enhanced permeability: AAPG Bulletin, v. 89, No.11, p.1493-1517.

Prothero, D.R., and F. Schwab, 1996, Sedimentary geology: An introduction to sedimentary rock and stratigraphy: W.H. Freeman and Company, San Francisco, p. 575.

Zhu, Q., A. C. Aller, F. Fan, 2006, Two-dimensional pH distributions and dynamics in bioturbated marine sediments: Geochimica et Cosmochemica Acta 70, p. 4933-4949.

Zorn, M.E., S. V. Lalonde, M. K. Gingras, S. G. Pemberton, K. O. Konhauser, 2006, Microscale oxygen distribution in various invertebrate burrow walls: Geobiology, v. 4, p. 1-9.

Chapter 2: The Petrographic Characteristics of Burrow-Associated Porosity Systems in Marine Sandstones

2.1 Introduction

As highly permeable conventional oil and gas reservoirs of North America near economic maturity, much attention is being drawn to unconventional reservoirs in finely-laminated and bioturbated sedimentary rocks (Law and Curtis 2002; O'Connell, 2003; Pederson, 2003). These sediments have localized porosity and permeability streaks within finer grained, mechanically compacted muddy rocks that can be artificially stimulated to produce hydrocarbons. Pemberton and Gingras (2005) point out that in the past, bioturbated rocks have been largely overlooked because they were viewed to have low bulk permeability. This is largely due to the churning action of burrowing macrofauna that effectively lower the grain sorting coefficient and hence permeability. Conversely, not much attention is given to bioturbation in intensely bioturbated rocks where high porosity and permeability have been preserved.

Simple observations made by petrographic analysis of burrowed marine sandstones provide an extremely informative first step in reservoir evaluation and prediction. It can provide an understanding of porosity and permeability heterogeneities and the geochemical evolution of early diagenetic reactions (eogenesis) that occur during the subsequent burial of the sediment. Authigenic mineral phases can be readily identified with common petrographic tools such as thin section analysis, x-ray diffraction (XRD), and scanning electron microscopy (SEM). Petrographic analysis

also provides fabric and textural evidence such as grain-size, grain-packing, and grain-shape that can lead to a reasonable burial history interpretation. As important, cement-dissolution (secondary porosity) porosity can be easily recognized by petrographic analysis. Criteria for the recognition of secondary dissolution fabric in thin sections of sandstones are provided in Schmidt and McDonald, (1979a); Schmidt, McDonald, and Platt (1977). Care must be emphasized as later diagenetic events related to uplift and unconformity proximity may show chemical replacement of original mineralogy and can lead to misinterpretation.

Wilson and Pittman, (1977) have shown that diagenetic reactions such as the precipitation of pore-filling carbonate and silica cements and authigenic clay can degrade reservoir quality, however little attention in the literature is given as to how bioturbation at or near the sediment-water interface can affect the eogenetic processes that will eventually affect the preservation of reservoir quality (Pemberton and Gingras, 2005). The recognition of these burrow-associated processes can be significant to oil and gas companies attempting to exploit hydrocarbons from marine sandstones as understanding porosity and permeability heterogeneities are key attribute to hydrocarbon production.

Invertebrate burrowing macroinfauna (including polychaete worms, crustaceans, amphipods, and meiofauna) can build extensive burrow systems within the upper 10-100 cm of the sediment column disrupting biogeochemical zones as the burrowing animals pass through or dwell

within these zones (Koretsky et al, 2002). Burrowing activities can have a major effect on sediment-water solute exchange and diagenetic reactions within the sediment because burrows can act as extensions of the sediment-water interface (Kristensen, 2001). Sediment can be disrupted by reworking of framework grains, irrigation activities, excretion, and grazing by burrowing fauna, which can result in extreme heterogeneities of the sedimentary matrix (Aller, 1994). Open burrows allow dissolved gasses to penetrate previously insulated pore water and sediment, altering the gas distributions within the sediment (Aller, 1988). Burrowing also affects Eh and pH distributions. For example, where burrows are present, Eh and pH distributions are highly heterogeneous and a wide range of biogeochemical reactions are possible and can change dramatically with depth (Zhu et al., 2006). The chemical reactions that occur within these biogeochemical zones are of central interest to this article as precipitation of eogenetic carbonate and silica cements and authigenic clay occur in these zones (Konhauser, 2007). The precipitation and dissolution of these cements can affect future reservoir quality of the sediment. Figure 2.1 shows an idealized representation of these biogeochemical zones. A partial range of burrow types and how they react with the biogeochemical zones is also shown.

The aim of this research is to illustrate the utility of petrography and to provide evidence of burrow-associated eogenetic alterations in several Cretaceous and Jurassic-aged marine sandstones using petrographic

techniques. In some cases, porosity is locally preserved in burrows that have undergone carbonate cement dissolution exceeding 15%, while other examples show almost complete reservoir occlusion by burrows filled with carbonate cement. Specific examples are used from the Cretaceous-aged Colony Sandstones and the Colorado Group bioturbated silty-shales of central Alberta, Canada as well as the Jurassic-aged Alpine Sandstones from the National Petroleum Reserve of Alaska to show how eogenetic carbonate cements affect reservoir quality.

Petrographic analysis is also important for recognising eogenetic silica cement. Examples have been chosen from the basal Banquereau Formation sandstones in the Hibernia oil field offshore Newfoundland, Canada and Jurassic-aged Khatatba Formation Sandstones in Egypt that show how early authigenic opaline cements can form and effect reservoir quality. These examples are compared to the Jurassic-aged Rock Creek Member and Nordegg Member of the Fernie Formation of central Alberta, Canada to show petrographic similarities in early quartz overgrowths that suggest these reservoirs have undergone eogenetic silica cementation due to burrow-associated early authigenic opal.

Petrographic identification of clay-filled porosity is extremely important as oil field wireline logs can detect high porosity in these zones, but this type of pore system yields little permeability (Serra, 1984). Experimental data by McIlroy et al (2003) have shown that ingested sediment can be altered in the guts of burrowing animals leaving porous

clay-filled burrows after the ingested material is excreted by the burrower's back-filling motion. Examples from the Aptian-age Ben Nevis/Avalon Formation Sandstones from the White Rose Oil Field, offshore Newfoundland, Canada and the Simpson Formation from the National Petroleum Reserve of Alaska are used to show how altered burrow associated eogenetic clay can affect reservoir quality.

All of the above examples were chosen because they are significant targets for oil and gas companies and they provide excellent examples of porosity heterogeneity caused by burrow-associated diagenesis. These examples are in no way a complete categorization of burrow-associated diagenesis and do not show complete formation or reservoir evaluation of the areas chosen, but do show that burrow-associated reservoir quality is wide spread and is common in the rock record and should not be ignored.

2.2 Methods

Twenty-five thin section samples from five formations were examined for this study. All petrographic thin sections used in this study were procured from the Suncor Energy Inc. (formerly Petro Canada Oil and Gas) thin-section database in Calgary Alberta, Canada. The samples were impregnated with a blue-dyed epoxy resin to identify porosity and to preserve pore-filling material. The samples were stained with Alizarin Red S to differentiate calcite and dolomite, and with potassium ferricyanide to

identify ferroan calcite and ferroan dolomite. Porosity and permeability data from core plugs were collected from industry sources. Minipermeametry data was taken from internal Suncor Energy Inc. data reports. Specific well names and depths have not been used to protect proprietary information. SEM and XRD data are from cited literature.

2.3 Burrow-Associated Early Carbonate Cements and Reservoir Quality

2.3.1 Colony Sandstone

Wickenden (1948) described the Colony sandstone as part of the Joli Fou Formation in the Colorado Group and considered it the uppermost unit of the Cretaceous-aged Mannville group; it was deposited in a restricted marine environment consists of coarsening upward deltaic quartzose sandstones. These sandstones are present throughout the subsurface of east-central Alberta, Canada and can provide a sizable natural gas reservoir where porosity is not occluded by early carbonate cement (Wickenenden, 1948). Petrographically this sand is of interest because it is evident that it has undergone eogenetic processes. Figure 2.2 shows an example of a highly burrowed Colony Sandstone sample. Close examination of the burrow shows the burrow fill to be coarser and cleaner sand than the burrow mantle. Though the burrow is completely filled with ferroan carbonate cement, original porosity of the burrow-fill is preserved in the cement. Note the undercompacted fabric of the quartzose sand inside the cemented burrow (Fig. 2.2B). Carbonate

cementation is aggressive to quartz grains due to the high alkalinity fluid it precipitates in (Friedman, 1976). This is evident as an *en echelon* texture in quartz grains that show the rhombohedral geometry of the carbonate cement in an attempt to recrystallize the quartz grain (Fig. 2.2C). Also, quartz grain embayment and corrosion textures are common (Fig. 2.2D). The muddy and finer grained area surrounding the burrow shows early stages of compaction indicating the overburden of buried sediment. The sand inside the burrow has been protected by the ferroan carbonate cement that has effectively supported the weight of overburden, and prevented the collapse of the framework grains. Though this sand has poor preserved reservoir quality it does provide useful petrographic evidence for carbonate cementation in rocks where carbonate cemented burrows have undergone subsequent dissolution.

2.3.2 Alpine Sandstones

The Alpine oil field is located in the National Petroleum Reserve in Alaska. Morris et al. (2000) describe the upper Jurassic-aged Alpine Sandstone as an informal member of the Kingak Formation. It is the stratigraphically highest sandstone within the Kingak Formation and is subdivided into the A and C unit. The A and C unit are divided by a regional unconformity. The Alpine A sandstone is stratigraphically lower and older than the C unit and consists of very fine to fine-grained, moderate to well sorted, burrowed, quartzose sandstone with variable

glauconite and clay content. Porosity is higher than 15%, but permeability can be less than 1 millidarcy owing to the microporous muddy matrix. The Alpine C sandstones are very fine to medium grained and are intensely bioturbated. Core porosity and permeability ranges are from 15% to 23% and 1 to 160 millidarcies respectively.

Figure 2.3 is an example of the Alpine A sandstone. This example is similar to the Colony sandstone example described above, but all of the cement within the burrow is dissolved. Petrographically it is evident that this burrow was originally cemented by carbonate. The undercompacted burrow-fill fabric, oversize pores in relation to grain size, grain embayment fabric, and remnant cement are all indications an earlier carbonate cement phase. The surrounding matrix rock shows indications of mechanical compaction due to burial, but the burrow fill shows evidence of undercompaction. This indicates that early carbonate cement precipitation enables the burrow fill to resist mechanical compaction leaving the sediment's original texture intact. The matrix rock suffers the permanent destruction of original porosity and permeability by compaction due to the ductile composition of the matrix and therefore collapses around the compaction resistant cemented burrow. During later burial diagenesis (mesodiagenesis) it is possible that acids generated by thermal break down of organic acids in adjacent mudrocks during hydrocarbon generation, dissolved the carbonate cemented burrows (Hendry, 2000). The chemistry of secondary porosity has been summarized elsewhere

(Surdam et al., 1984). Spot permeametry taken from the unburrowed portion of core has 0.01 millidarcies of permeability where as the burrowed sand is four orders of magnitude higher at 60 millidarcies.

Figure 2.4 is an example taken from the Alpine C Sandstone. This sand is extremely bioturbated and coarser grained with a measured porosity at 18% and permeability of 82.3 millidarcies. The matrix has been replaced by siderite. This may indicate that early sulphate reduction caused the matrix to be replaced by siderite, but more importantly the sulphate reduction reaction may have been the source of the carbonate cement that originally cemented the burrows and protected them from the affects of mechanical compaction during the subsequent burial of the sediment.

2.3.3 Colorado Silts and Shales

Robinson et al., (2008) described The Cretaceous-aged Upper Colorado Group siltstones and shales of central Alberta, Canada as being deposited in a distal marine setting, laterally extensive and can be hundreds of meters thick, and much of the natural gas in these rocks is biogenic methane. These finely laminated and bioturbated rocks can be artificially stimulated to produce low-rate gas that may produce for decades. Figure 2.5 is an example of bioturbated Colorado Group silty shale. Close examination of the burrows show evidence of carbonate dissolution. The burrows have all resisted the effects of mechanical

compaction indicating that they were likely filled with early carbonate cement. In Figure 2.5A a pyrite-filled burrow is present which indicates a reducing environment. It is possible that the carbonate cement that filled the burrows was sourced from the sulphate reduction zone. Acids that are associated with the on-set of hydrocarbon migration may have dissolved the cement and the burrows provide a permeable conduit for gas storage once complete dissolution has occurred.

2.4 Burrow-Associated Early Silica Cement and Reservoir Quality

2.4.1 Khatatba Sandstones

Goldstein and Rossi (2002) have shown by using special petrographic techniques such as SEM-cathodoluminescence that the quartz overgrowths in the Jurassic-aged Khatatba Formation Sandstones in Egypt are likely formed from early phase opaline silica. The quartz overgrowths in the Khatatba sands are in optical continuity and appear typical under transmitted light (Fig. 2.6). The same quartz overgrowths examined under cathodoluminescence show textures that can be interpreted as recrystallization fabric. These fabrics clearly show that initial precipitation was not quartz overgrowths with simple planar terminations, but as fine bands and fibrous blades indicating that the silica cementation had undergone stages of precipitation from opal-A to opal-CT. Figure 2.6 also shows the final stage of the quartz overgrowth that forms the outer portion that may be consistent with the opal-CT to quartz stage.

2.4.2 Banquereau Formation Sandstones

Early opaline cements were found in the non-reservoir basal Tertiary Banquereau Formation sandstones in the Hibernia oil field offshore Newfoundland, Canada. These porcellanites contain pervasive opal-CT cements that were substantiated by thin section, SEM, and XRD analysis (Fig. 2.7). The authigenic cements are dominated by silica (opal-CT, chalcedony and microquartz). The opal-CT occurs as early grain-rimming lepispheres and as pore-filling masses of coalesced lepispheres. This is a very important petrographic observation as this zone showed a high pay porous zone on wireline logs, but all the porosity was ineffective microporosity within the microporous lepispheres. Chalcedony occurs as fibrous pore-filling cement and microquartz is a final phase cement restricted to fracture-fill. It is evident from the petrographic evaluation that the original porous sediment was initially filled with opal-A then replaced by opal-CT (as lepispheres). With progressive silicification (following the steps of Ostwald ripening) the lepispheres enlarge and eventually fill the pore space (Ratke et al., 2002). Within the interval examined, the volume of opal-CT cement suggests a low terrigineous sediment input and/or high biomass productivity. This may reflect an early influence of cold, nutrient-rich water in mid Eocene times.

2.4.3 Fernie Formation Sandstones

Figure 2.8 shows an example from the shoreface sandstones of the Jurassic-aged Nordegg Member of the Fernie Formation from central Alberta, Canada. This arenitic sandstone shows evidence of strong bioturbation. The sand within the burrow is almost completely silica cemented with minor amounts of ferroan carbonate cement. Closer petrographic investigation shows that the quartz overgrowths show chalcedonic early fabric as dark brown rims on the quartz overgrowths similar to that of the Khatatba Formation Sandstones and from the Banquereau Formation samples mentioned above. The reservoir quality of this sandstone has been severely reduced by silica cement. It is likely that the animal burrowing through this sand cleaned the mud out allowing the flow of silica enriched fluids that precipitated the silica cement.

Figure 2.9 shows an example from the Jurassic-aged Rock Creek Member of the Fernie Formation from central Alberta, Canada. This example is very similar to the Nordegg example, and silica cementation within the burrows shows the same early fabric as in the Nordegg. In this case, the Jurassic sandstones were likely never hydrocarbon charged as the silica cement precipitated shortly after the burrowing event. Both the Nordegg and Rock Creek members of the Fernie Formation have shown excellent reservoir quality preservation in shoreface sandstones capable of producing gas at economical rates, but careful facies mapping of these sands is necessary to avoid the burrow-associated silica cemented sands.

2.5 Burrow-Associated Early Authigenic Clay and Reservoir Quality

Experiments by McIlroy et al (2003) have shown that weathering and low temperature authigenesis are influenced by bioturbation. Low pH digestive processes in the guts of the annelid *Arenicola marina* degraded metamorphic chlorite and muscovite and caused the growth of neoformed authigenic clays. Identical experimental tanks were used, one with the annelid and the other as a control. The sand, mud, and seawater were identical in both tanks. The sand was clay free and the mud was composed of crystalline muscovite and chlorite as demonstrated by XRD analysis. XRD traces show a neoformed mineral not present in the control tank that corresponds to the mineral berthierine (McIlroy et al., 2003).

2.5.1 Ben Nevis/Avalon Member Sandstones

Figure 2.10 shows an example from the offshore White Rose Oil Field located in the Jeanne d'Arc Basin approximately 350 km east of St John's, Newfoundland, Canada. A well preserved burrow in the Aptian-age Ben Nevis/Avalon Formation sandstone reservoir rock shows the back-fill nature of the burrower. A closer look at this burrow shows chlorite filled porosity. This portion of the thin section has high porosity (12%), but very low permeability (0.05 millidarcies). This sample is not from the producing zone, but shows an excellent example of how clay-filed burrows affect reservoir quality.

2.5.2 Simpson Sandstones

Bayliss and Syvitski (1982) found that fecal pellets are, in general, composed of the same material as the bulk of the seafloor, except in the case where degraded illite and biotite has adsorbed Fe and K to regrade into glauconite. This shows that diagenetic minerals commonly associated with burial can be produced by sediment-organism interactions.

Houseknecht and Bird (2004) describe the Simpson sandstones within the Jurassic Kingak Shale in the National Petroleum Reserve of Alaska consisting of muddy glauconitic sandstones. These sandstones have porosities in excess of 20% but permeabilities rarely above 1 millidarcy. Figure 2.11 is an example of the glauconite-rich Simpson Sandstone. In this example partial to almost complete dissolution of glauconite grains leaves high porosity, but this porosity is largely ineffective microporosity and permeability of this sandstone is low. These glauconite grains were likely faecal casts as those mentioned above.

2.6 Discussion

Burrow-associated eogenetic reactions can have a dramatic effect on the future reservoir quality of marine sandstones as shown in the examples above. The decomposition of organic matter plays an extremely important role in creating biogeochemical microenvironments where eogenetic minerals can form (Konhauser, 2007). Burrowing marine invertebrates can disturb the biogeochemical environments by extending

the well oxygenated sediment-water interface and the burrow linings may provide excellent nucleation sites for eogenetic cements to form (Aller, 1988). Of these cements carbonates, silica, and authigenic clay are the most dominant mineral phases in siliciclastic rocks.

2.6.1 Carbonate Cement

The first reactive pathway for the degradation of organic carbon is at the sediment-water interface (Konhauser, 2007). This reaction is shown by:

$$C_6H_{12}O_6 + 6O_2 \rightarrow 6CO_2 + 6H_20$$

CO_2 and H_2O further react to form HCO_3^- by the following simple reaction:

$$CO_2 + H_2O \leftrightarrow H_2CO_3$$

$$H_2CO_3 \leftrightarrow H^+ + HCO_3^-$$

HCO_3^- is then released into the pore system increasing alkalinity and hence precipitation of early diagenetic carbonates by anaerobic processes by the following:

$$HCO_3^- + Ca_2^+ \leftrightarrow CaCO_3 + H^+$$

$$Ca_2^+ + CO_3 \leftrightarrow CaCO_3$$

If there is an abundance of Mg^{2+} in the pore water dolomite precipitation can occur.

$$Ca_2^+ + Mg^{2+} + CO_3 \leftrightarrow CaMg\,(CO_3)_2$$

Once these cements have nucleated, carbonate cementation can rapidly fill all of the available pore space and become extremely stable.

In suboxic zones, nitrate reduction does not form calcium carbonate, but rather siderite, pyrite, and in some cases rhodochrosite (Morad, 1998). In the anoxic sulphate reduction zone nonferroan calcite can form in the presence of hydrocarbon and anhydrite by the following:

$$\underset{\text{Hydrocarbon}}{CnH_2n} + \underset{\text{Anhydrite}}{CaSO_4} \rightarrow \underset{\text{Methane}}{CH_4} + H_2O + H_2S + CO_2 + \underset{\text{Calcite}}{CaCO_3}$$

It is in this zone where H_2S gas is formed. Pyrite can form in the presence of sulphate reducing bacteria and Fe in solution. Early diagenetic siderite can form in low sulphide concentration with high dissolved carbonate, low Eh, and neutral pH. These conditions usually restrict siderite to non-marine environments, but these conditions do occur in shallow marine environments. Siderite forms after organic matter decomposition by nitrate-manganese-iron reduction otherwise pyrite formation will be favoured (Stonecipher, 1999).

2.6.2 Silica Cement

It has often been viewed that quartz cementation can only occur during deep burial processes at high temperature (Tucker, 2001). However, it is possible due to thermodynamic and kinetic controls to precipitate silica cement at low temperatures in a closed system. This type of silica precipitation requires the dissolution and reprecipitation of silica that takes place during sedimentation of siliceous eukaryotic debris (Konhauser, 2007). The silica is diagenetically altered and recycled

throughout the sediment. Benthic communities aid in mixing the siliceous tests within the sediment and enrich pore waters with silica. Once the dissolved silica enters the pores it can then precipitate as opal-A (amorphous silica). Amorphous silica can dissolve and reprecipitate as opal-CT (disordered crystobalite-tridymite) and with depth, transforms to quartz. This is a spontaneous redistribution of mass from smaller precursor silica to larger phases known as Ostwald ripening. Ratke et al. (2002) have shown that Ostwald ripening is a thermodynamically driven spontaneous process in which larger particles are more energetically preferred over smaller less stable particles over a period of time. As the system lowers its overall energy, molecules on the surface of the small particle will diffuse through solution and add to the large particle; the smaller particles shrink while the larger particles grow provided a supply of the mineral is constant.

Once the siliceous eukaryote debris has reached the sea bottom sediment, it is then exposed to bioturbation. Oxygen and organic matter play important roles in the type and size of the benthic community present. If oxygen and/or edible organic matter is strongly depleted the benthic communities will be restricted. As the burrowing animals search for food, they can cause a mixing of opaline debris into the substrate. Dissolution of the opal proceeds within the sediment (van der Weijden, 2007). The benthic flux of silicic acid can be measured directly or can be calculated from pore water profiles of dissolved silicon (McManus et al, 1995; Sayles

et al., 1996; Zorn et al., 2006) show good examples of the methods used to measure benthic fluxes in ideal conditions.

2.6.3 Authigenic Clay

No study of diagenesis is complete without a discussion of clay minerals. Clay minerals include kaolinite, illite, interstratified mixed layer clays, smectite, and chlorite. These minerals play an important role in early siliciclastic diagenesis. Clays can be difficult to identify with thin sections alone owing to the extremely small grain size. More advanced petrographic techniques are utilized in identifying these types of minerals. Scanning electron microscopy (SEM) in conjunction with energy dispersive spectrometry along with semi-quantitative X-ray diffraction (XRD) can provide adequate clay mineral identification. Without adequate petrographic analysis of available core or drill cuttings these clays are left undetected until the well in question will not produce expected hydrocarbon rates.

2.7 Conclusions

Several thin section samples from various hydrocarbon reservoirs were used to show the porosity heterogeneities that can develop due to burrow-associated diagenesis. Petrographic technique was used to show that within these marine sandstones authigenic mineral identification and

rock fabric/textural observations can lead to a better understanding of the porosity heterogeneities that control reservoir quality.

Diagenetic processes begin at the instant of deposition. Biogeochemical heterogeneities at the sediment-water interface can be dramatic, and bioturbation by benthic fauna can further complicate this environment. Burrowing fauna continually irrigate and oxygenate sediments as they burrow. Introduction of fresh organic matter, such as planktonic debris, can stimulate the decomposition of stable buried organic carbon-rich sediment. This is achieved as burrowers periodically intermix the organic matter with oxygen. Bioturbated organic carbon-rich sediments constantly undergo oscillations between oxic and anoxic conditions. Oxygenated waters can then be introduced to previously isolated pore water. This allows for re-oxidation of reduced metabolites. Pore water pH distributions are closely related to early diagenetic reactions and transport processes. When burrows are present, pH distributions are highly heterogeneous.

Geochemically altered microenvironments can occur syndepositionally with burrowing up to centimetres from the burrow walls. These microenvironments may provide early nucleation sites for diagenetic cements to precipitate or dissolve. This has great implications on the future reservoir quality of these depositional environments as porosity and permeability can be severely affected by the precipitation and/or dissolution of these early diagenetic cements.

Carbonate cement is one of the most common pore occluding cements in sandstones and can severely reduce the reservoir quality; however, recoverable secondary porosity due to dissolution of carbonate cement can leave an oversized pore system, increasing permeability and reservoir quality especially if the sand has been bioturbated previously. Silica cementation is also one of the most important pore-occluding authigenic mineral phases effecting reservoir quality in marine and marginal marine sandstones. Through the spontaneous kinetic reactions of Ostwald ripening, it has been shown in various cases that early opaline cements can indeed be responsible for pore occluding silica. Recognition of early silica is important because it is an early phase of cement and the pore system was likely never hydrocarbon charged and original porosity is non-recoverable. Petrographic identification of pore-filling authigenic clay is equally important. Pore-filling clay can retain porosity as ineffective microporosity, but permeability is very low.

Careful examination of these fabrics and mineral identification is essential to assessing reservoir quality in burrowed hydrocarbon reservoirs. Detailed ichnological core work can lead to a better understanding of the depositional environments that contained trace fossil makers. Marine and marginal marine environments can have great lateral extent, be predictable, and are mappable, therefore detailed petrographic work is crucial to understanding and predicting the diagenetic sequence in which authigenic minerals were precipitated and/or dissolved.

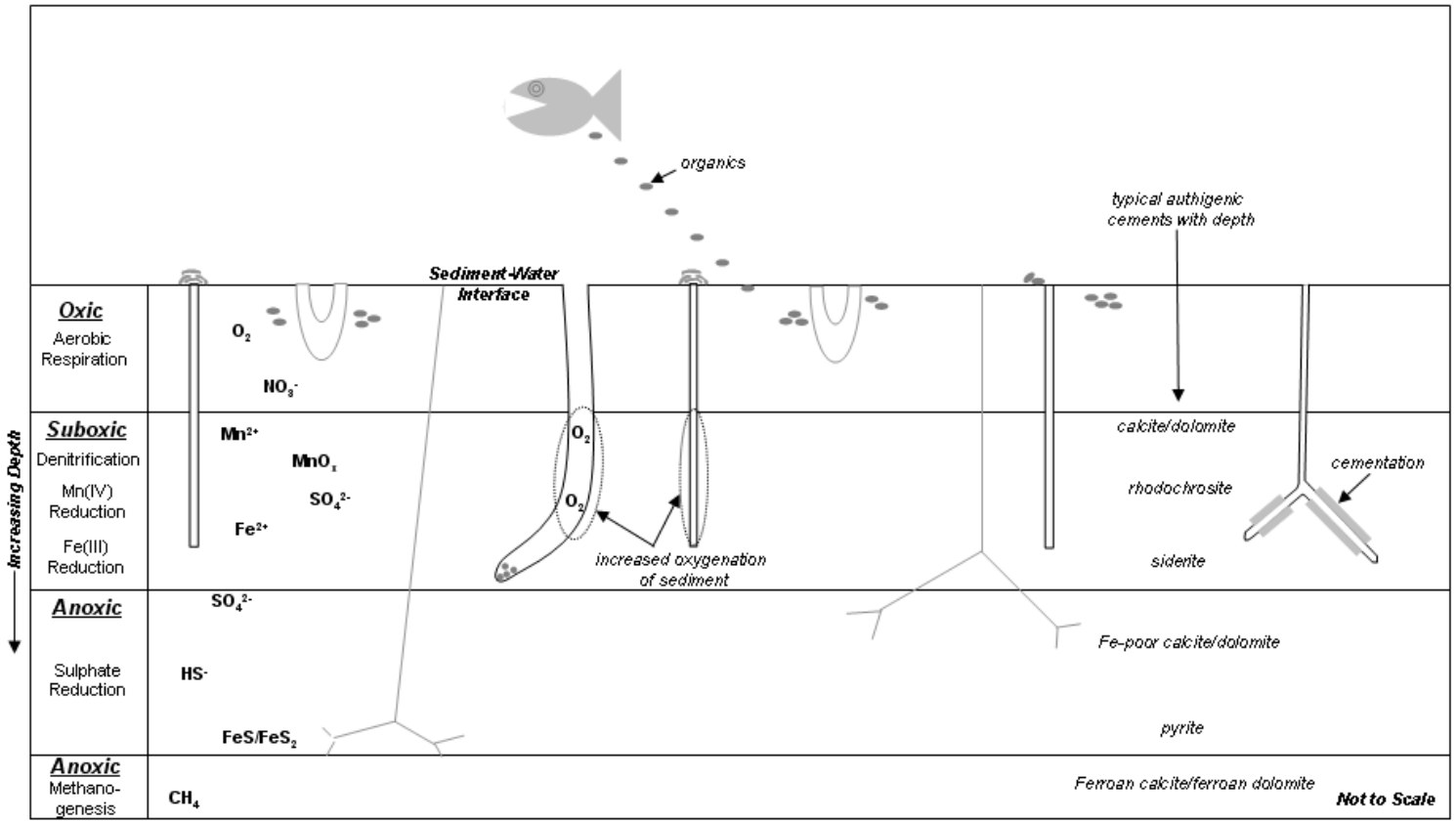

Figure 2.1 Biogeochemical zones of organic-inorganic interactions with burial depth of organic matter and marine siliciclastic sediment. A partial range of burrow types have been added to show how they react within the oxic, suboxic, and anoxic zones. Note how burrows can act as extensions of the sediment-water interface allowing oxygen and other nutrients to penetrate previously depleted zones. Typical authigenic carbonate cements that can precipitate in these zones are shown. The actual thickness of each zone is largely dependant on sedimentation rate (modified from Konhauser and Gingras, 2007; Morad, 1998; Berner, 1991; and Hesse, 1990).

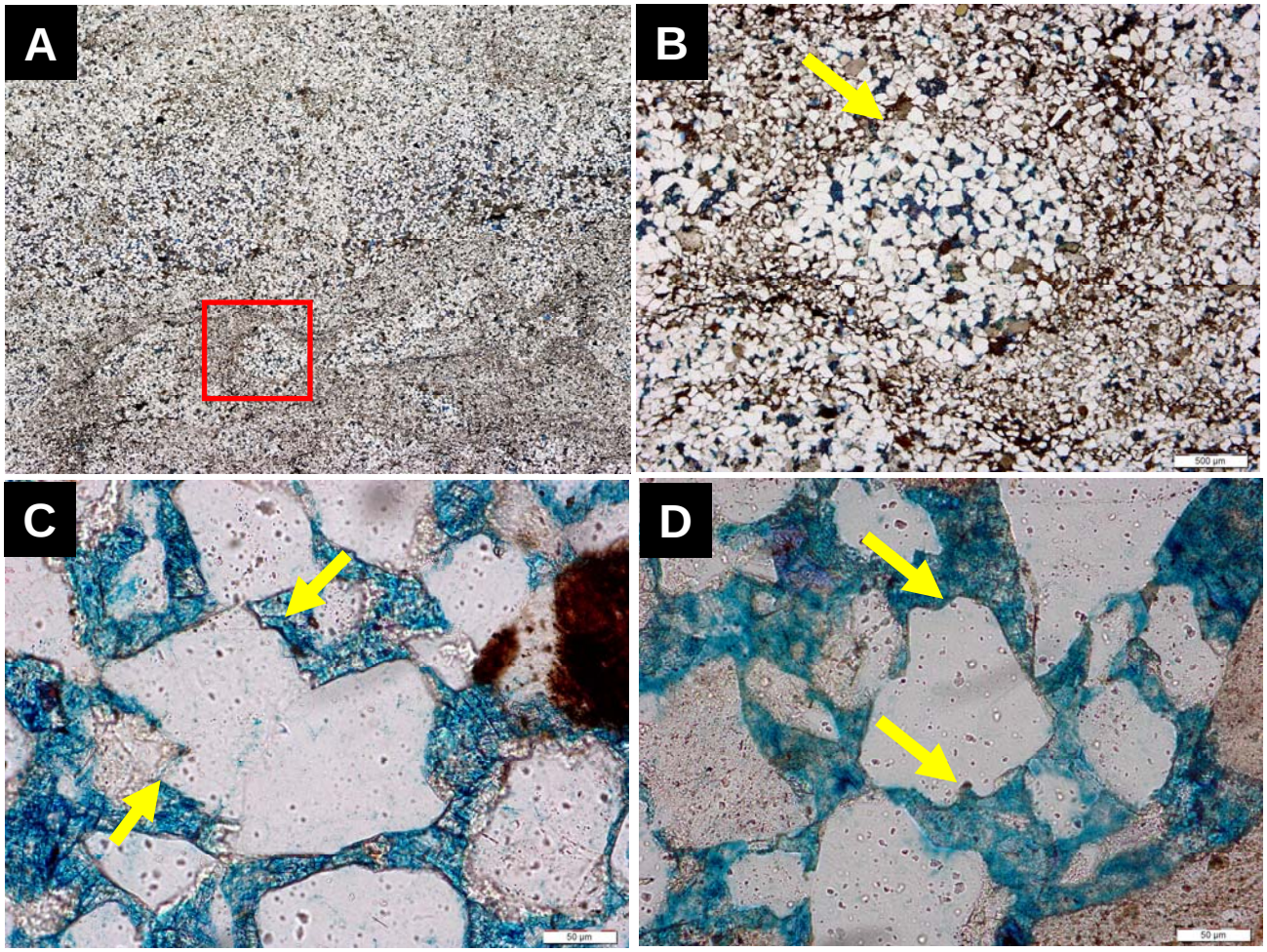

Figure 2.2 (A) Overview scan of a burrowed Colony Sandstone thin section sample (Field of view (FOV) approximately 2.5 cm wide). (B) Closer view of burrow highlighted by the red box in photo (A) showing the complete porosity occlusion by ferroan carbonate cement inside a burrow (arrow). Note the undercompacted fabric of the quartzose sand inside the cemented burrow (scale bar is 500 microns). The muddy and finer grained area outside the burrow shows early stage of compaction (centre of frame). (C) The en-echelon texture to quartz grain (arrow). This texture is due to the rhombohedral geometry of the carbonate cement (scale bar is 50 microns). (D) Grain embayment texture (arrows) (scale bar is 50 microns). These textures are preserved in samples where complete dissolution has taken place leaving behind clues of an earlier cementation event.

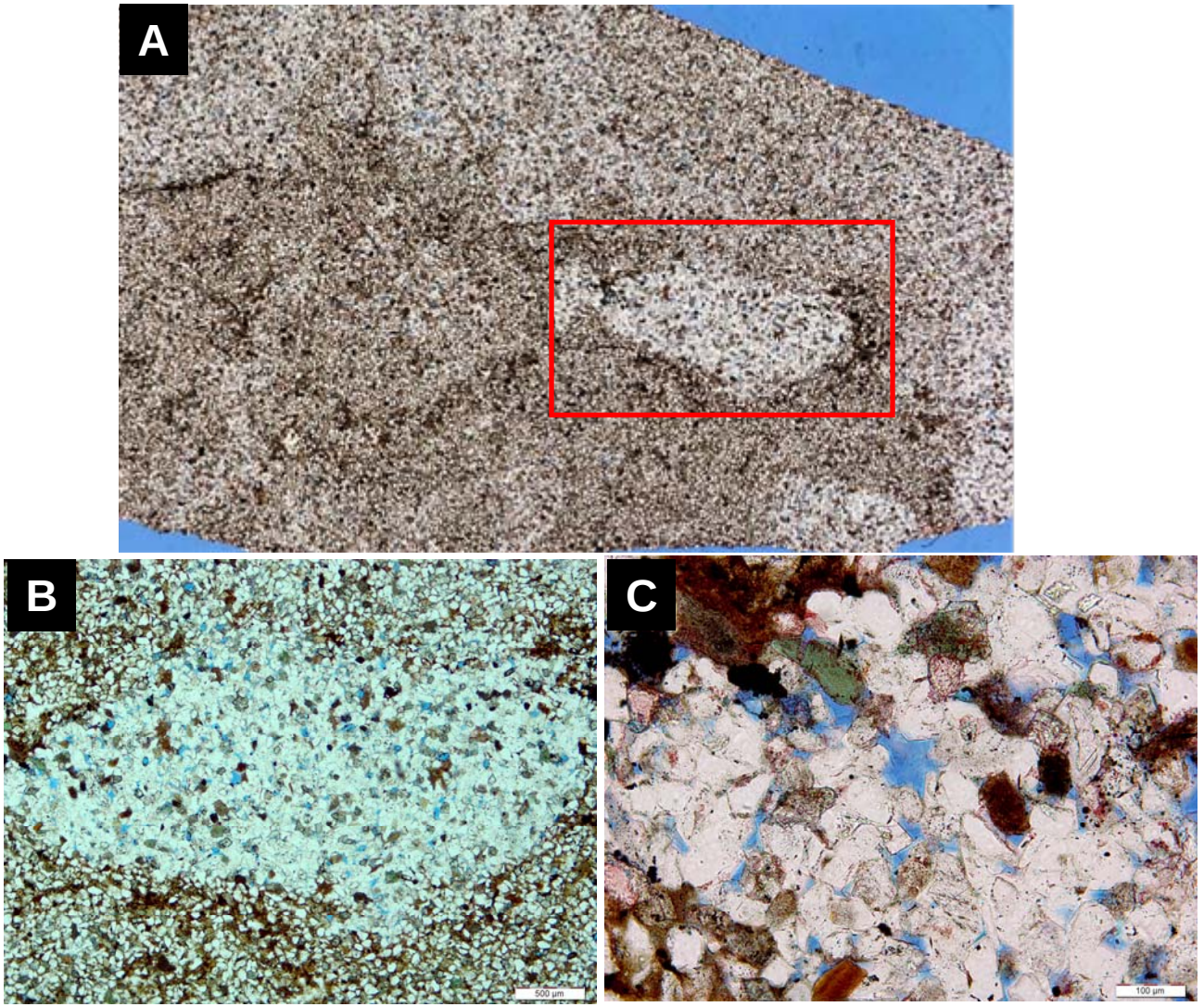

Figure 2.3 (A) Thin section overview of a very fine grained argillaceous sandstone from the Jurassic-aged Alpine A sandstone from the NPRA (FOV approximately 2.5 cm wide). This sample has low bulk permeability (Kmax = <0.01millidacies). (B) Closer view of burrow highlighted with the red box in photo (A) (scale bar is 500 microns). (C) Illustrates the dissolution of carbonate cement preserving original porosity. Note the undercompacted fabric inside burrow. The sand in this burrowed area has four orders of magnitude better permeability (60 millidarcies) than the matrix sand (scale bar is 100 microns).

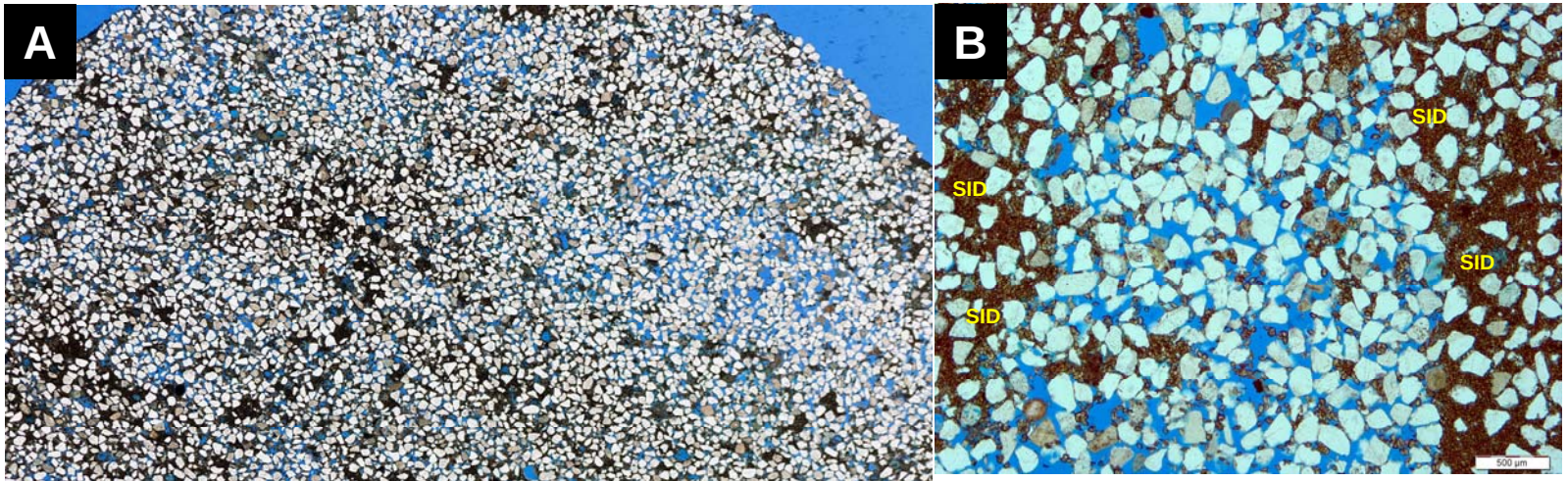

Figure 2.4 (A) Thin section overview of a fine grained sandstone from the Jurassic-aged Alpine C sandstone from the NPRA (FOV approximately 2.5 cm wide). (B) Closer view of burrow highlight with the red box in photo A (scale bar is 500 microns). This photo shows the muddy matrix has been completely replaced by siderite (SID) and the burrow has undergone complete carbonate cement dissolution. Note that the quartz grains are very loosely packed and are in point-to-point contact. This is evidence of original burial porosity. Porosity = 18% and permeability is 82.3 millidarcies.

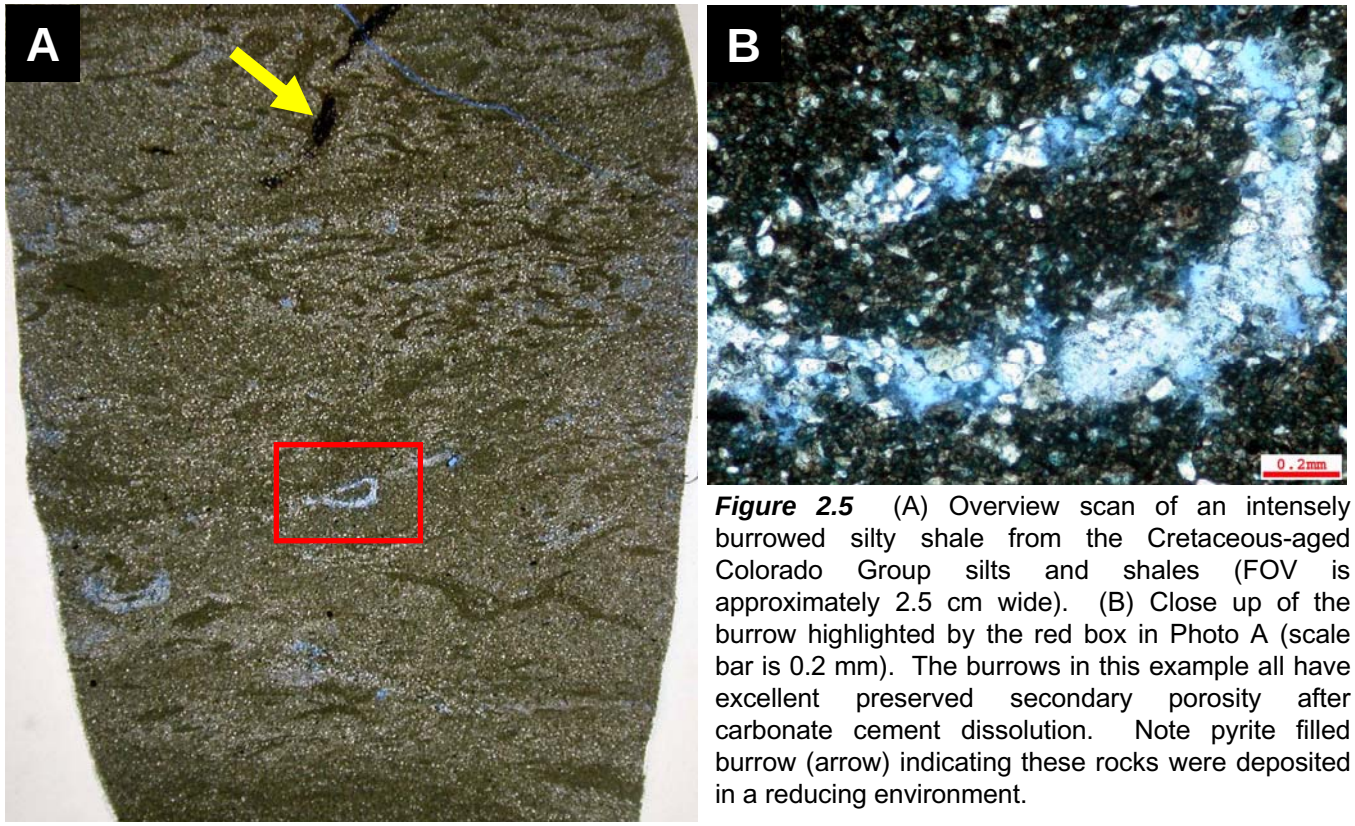

Figure 2.5 (A) Overview scan of an intensely burrowed silty shale from the Cretaceous-aged Colorado Group silts and shales (FOV is approximately 2.5 cm wide). (B) Close up of the burrow highlighted by the red box in Photo A (scale bar is 0.2 mm). The burrows in this example all have excellent preserved secondary porosity after carbonate cement dissolution. Note pyrite filled burrow (arrow) indicating these rocks were deposited in a reducing environment.

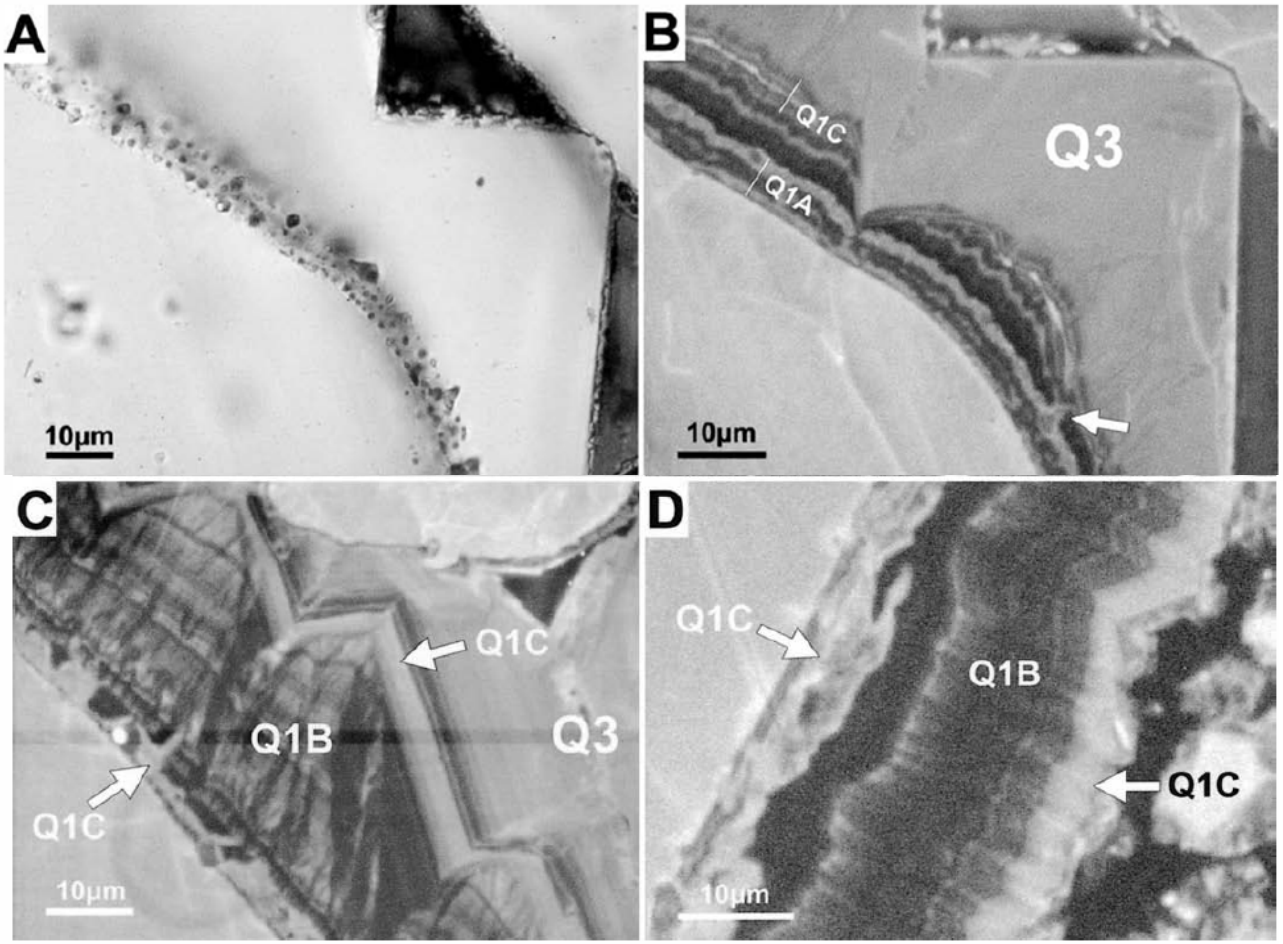

Figure 2.6 Photomicrographs of quartz overgrowth in plane-polarized light. (A) Overgrowth appears optically continuous, bearing no hint of internal structure. (B) Same field of view as A, but under SEM-CL. Q1A and C show earlier precipitation of opal-CT. Q3 is a later phase of quartz. (C) Q1B shows banded fabric of opal-CT. Q1C preferentially fills area near base of overgrowth, but morphologies of wall do not match along opposite sides of area filled with Q1C. (D) Q1B preserves "ghosts" of fibrous structures (from Goldstein and Rossi, 2002).

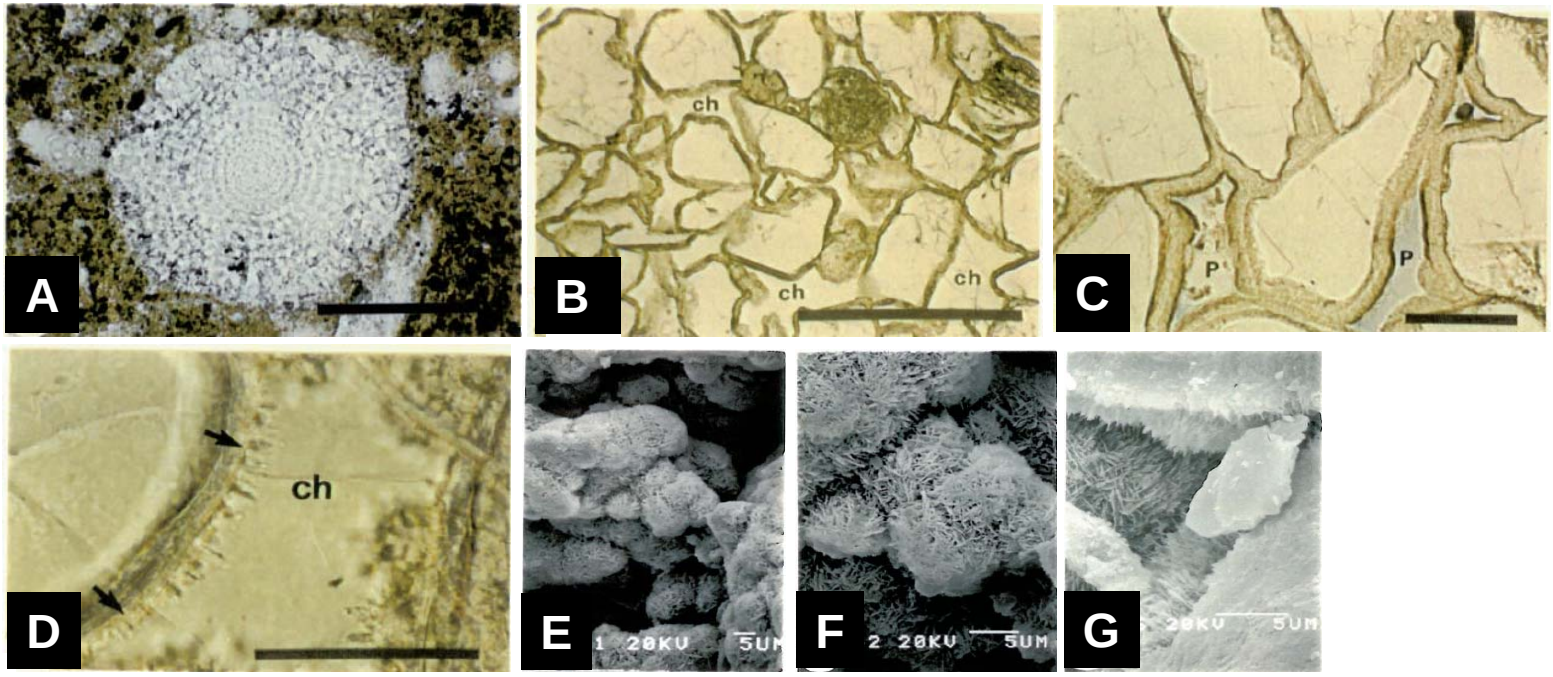

Figure 2.7 (A) Well preserved siliceous radiolarian test; scale bar = 0.1mm. (B) Quartz arenite with well developed opal-CT rims on detrital grains and complete pore occlusion by chalcedony cement (ch); scale bar = 0.5mm . (C) Close view of grain-rimming lepispheric opal-CT. Some pores are still preserved (P); scale bar = 0.1mm. (D) Close view of pore completely filled with chalcedony (ch); scale bar = 0.05mm . Note bladed fabric (arrows). (E) (F) and (G) SEM photomicrographs of lepispheres (Meloche, 1984).

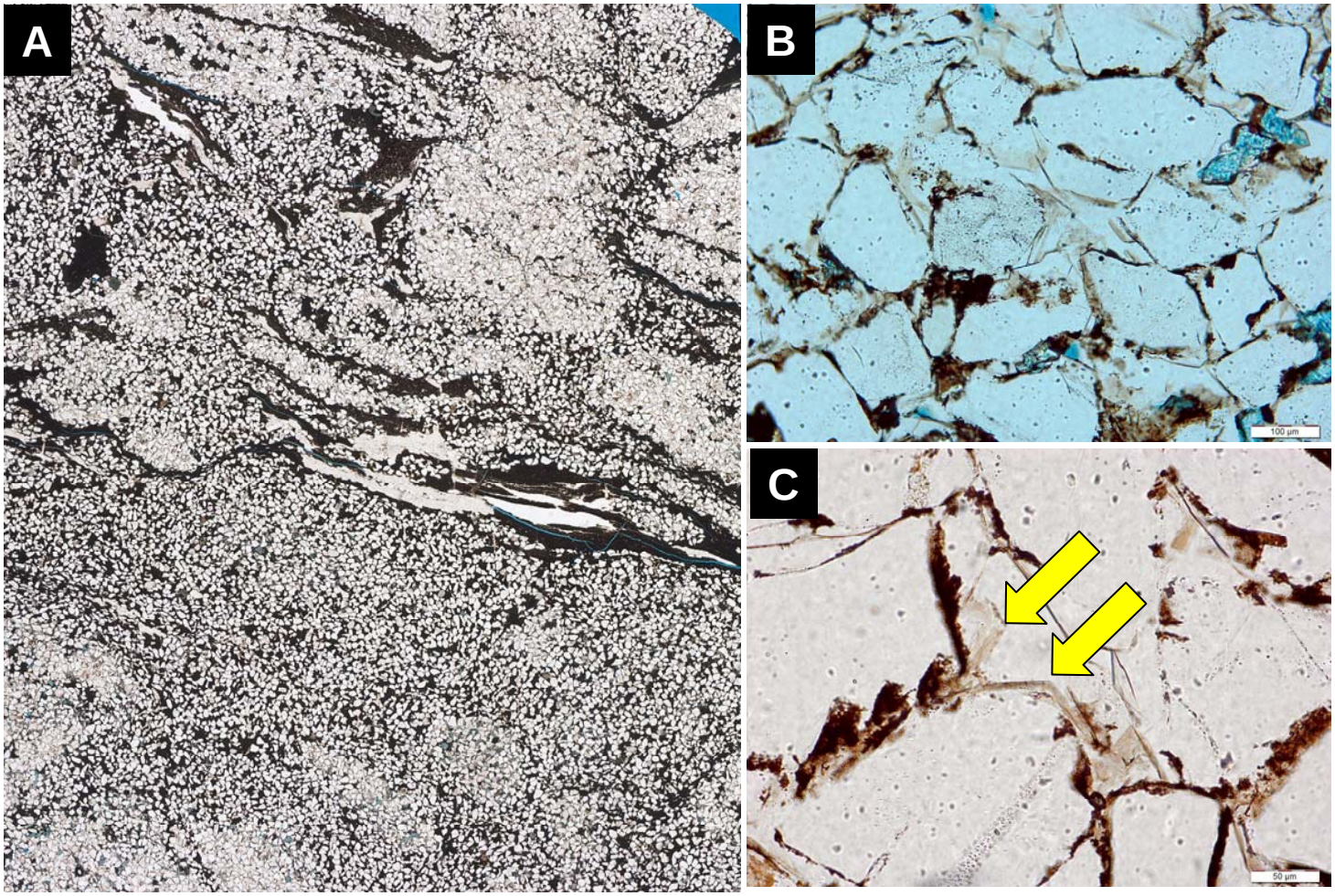

Figure 2.8 (A) Overview thin section scan from the shoreface sandstones of the Jurassic-aged Nordegg Member (FOV approximately 2.5cm wide). (B) Sand within the burrow is almost completely silica cemented with minor amounts of ferroan carbonate cement (scale bar is 100 microns). (C) Quartz overgrowths show chalcedonic early fabric (arrow) similar to that of the Khatatba Formation Sandstones and from the Banquereau Formation samples (scale bar is 50 microns). The reservoir quality if this sandstone has been severely reduced by silica cement.

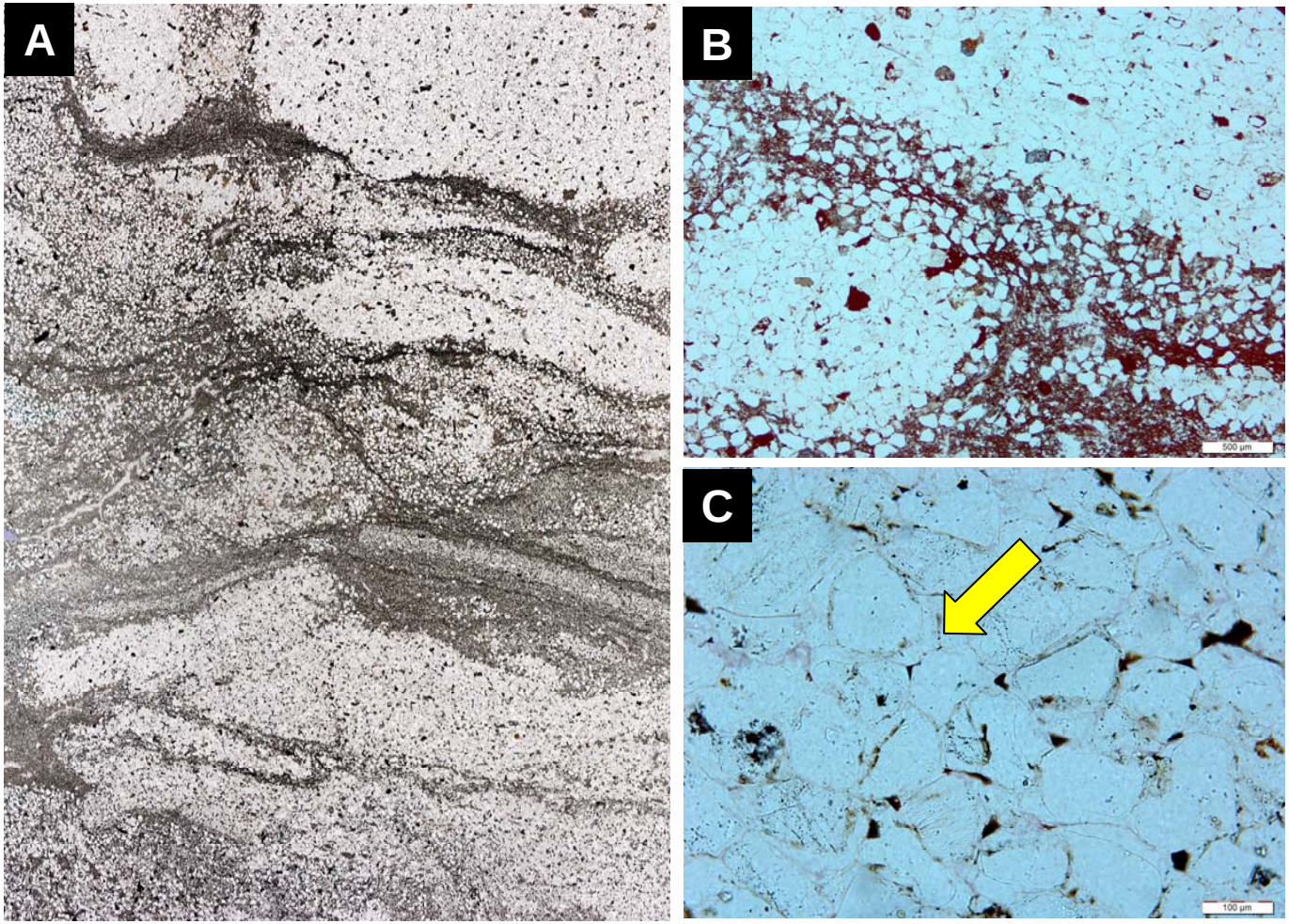

Figure 2.9 (A) Overview thin section scan from the shoreface sandstones of the Jurassic-aged Rock Creek Member (FOV approximately 2.5 cm wide). (B) Closer view of the silica cemented burrows (scale bar is 500 microns). (C) Quartz overgrowths show chalcedonic early fabric (arrow) similar to that of the Khatatba Formation Sandstones, the Banquereau Formation samples and from the previous Nordegg sample (scale bar is 100 microns).

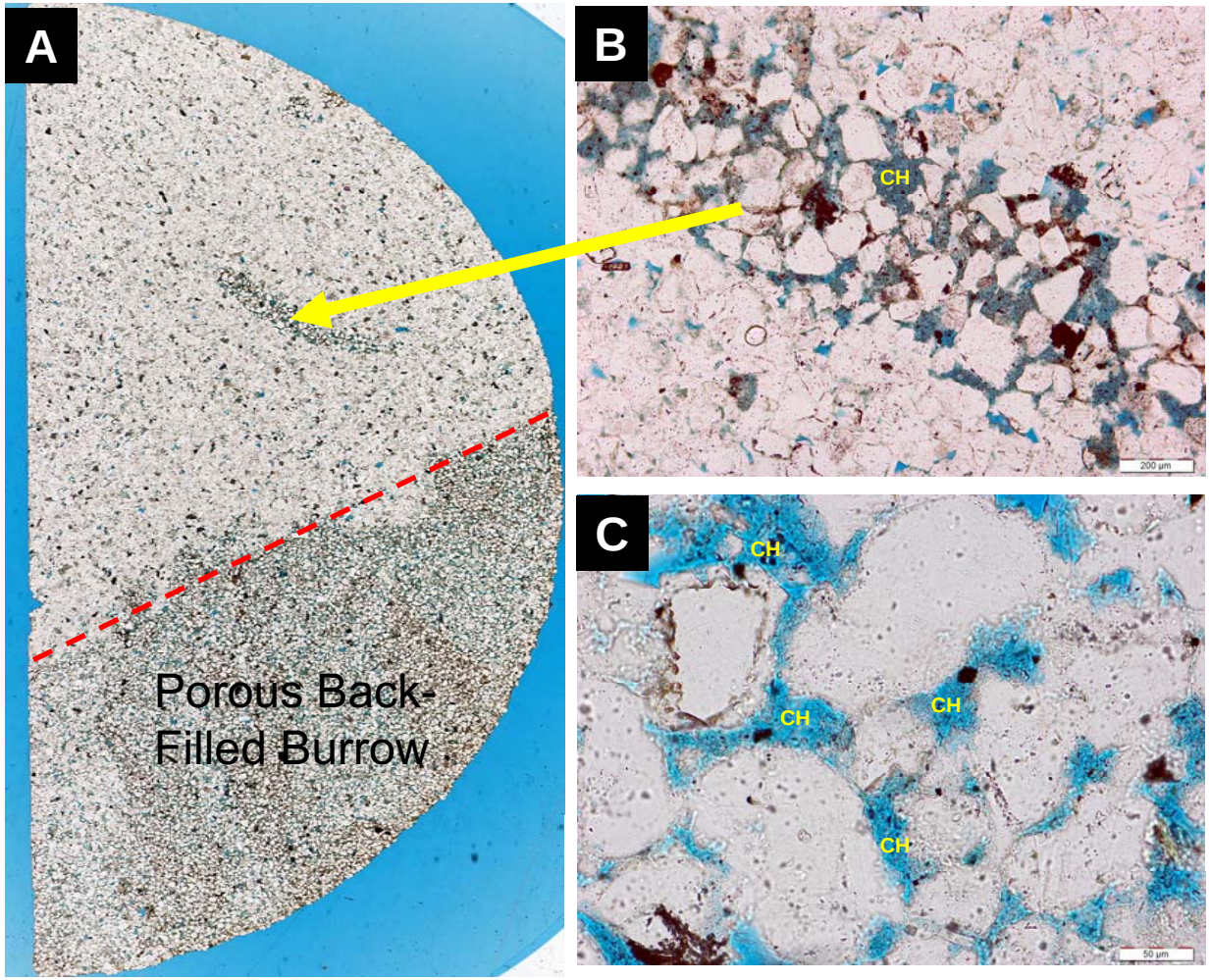

Figure 2.10 (A) Overview thin section scan example from the Ben Nevis/Avalon Formation sandstone (FOV approximately 2.5 cm wide). A well preserved burrow shows the back-fill nature of the burrower. (B) (scale bar is 200 microns) and (C) (scale bar is 50 microns) show a closer look at this burrow showing chlorite (CH) filled porosity. This portion of the thin section has high porosity (12%), but very low permeability (0.05 millidarcies).

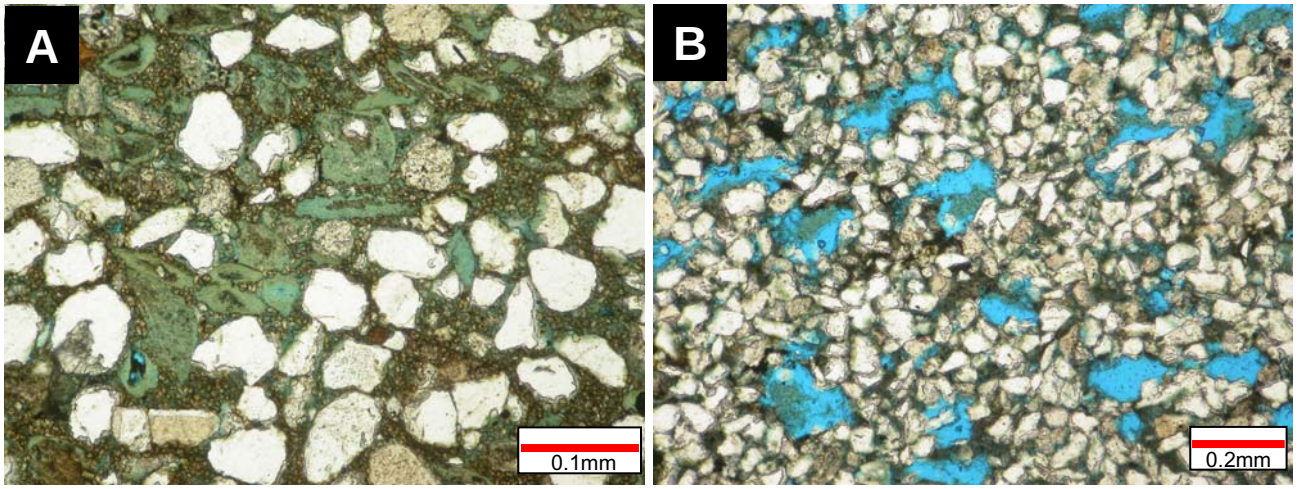

Figure 2.11 (A) Glauconite-rich sandstone from the Simpson Sandstone in the NPRA. Porosity is high due to microporosity in glauconite, but permeability is low. (B) Simpson Sandstone showing almost complete dissolution of glauconite. This sample has high porosity, but low permeability as pores are not well connected.

2.8 References

Aller, R.C., 1988, Benthic fauna and biogeochemical processes in marine sediments: the role of burrow structures, Scope (Chichester) 33, p. 301-338.

Aller, R.C., 1994, Bioturbation and remineralization of sedimentary organic matter: effects of redox oscillation, Chemical Geology 114, 1994, p. 331-345.

Bayliss, P., and P. M. Syvitski, 1982, Clay diagenesis in recent marine fecal pellets: Geo Marine Letters, volume 2, numbers 1-2, p. 83-88.

Berner, R.A. 1980, Early Diagenesis: a theoretical approach: Princeton University Press, Princeton, N.J., p 241.

Friedman, G. M., A. A. Syed., 1976, Dissolution of quartz accompanying carbonate precipitation and cementation in reefs: example from the Red Sea. Journal of Sedimentary Research, v. 46, p. 970-973.

Goldstein, R.H. and C. Rossi, 2002, Recrystallization in quartz overgrowths: Journal of Sedimentary Research, v. 72, p. 432-440.

Hendry, J. P., M. Wilkinson, A. E. Fallick, and R. S. Haszeldine, 2000, Ankerite Cementation in Deeply Buried Jurassic Sandstone Reservoirs of the Central North Sea: Journal of Sedimentary Research, v.70, p. 227 - 239.

Hesse, R., 1990, Origin of chert: diagenesis of biologic siliceous sediments: In McIlreath, I.A., and Morrow, D.W., eds, Diagenesis: Geological
Association of Canada, Geoscience Canada, Reprint Series 4, p. 227-275.

Houseknecht, D. W., and K. J. Bird, 2004, Sequence stratigraphy of the Kingak Shale (Jurassic–Lower Cretaceous), National Petroleum Reserve in Alaska: AAPG Bulletin, v. 88, no. 3, p. 279-302.

Konhauser, K.O., 2007, Introduction to Geomicrobiology: Blackwell Publishing USA, p. 262-292.

Konhauser, K.O. and M. K. Gingras, 2007, Linking geomicrobiology with ichnology in marine sediments: Palaios, v. 22, p.339-342.

Koretsky, C.M., C. Meile, P. Van Cappellen, 2002, Quantifying bioirrigation using ecological parameters: a stochastic approach. Geochemical Transcripts, 3, p 17-20.

Kristensen, E., 2001, Impact of polychaetes (Nereis spp. and Arenicola marina) on carbon biogeochemistry in coastal marine sediments: Geochemical Transcripts, v.2, p. 92–103.

Law, B. E., and J. B. Curtis, 2002, Introduction to unconventional petroleum systems: AAPG Bulletin, v. 86, p. 1851-1852.

McIlroy, D., R. H. Worden, S. J. Needham, 2003, Faeces, clay mineral and reservoir potential: Journal of the Geological Society, London, vol. 160, p 489-493.

McManus, J., D. E. Hammond, W. M. Berelson, T. E. Kilgore, D. J. DeMaster, G. Ragueneau, R. W. Collier, 1995, Early diagenesis of biogenic opal: Dissolution rates, kinetics, and paleoceanographic implications, Deep-Sea Research II, v.42, p. 871–903.

Morad, S., 1998, Carbonate cementation in sandstones: distribution patterns and geochemical evolution. International Association of Sedimentologists, Special Edition Number 26, p. 1-26.

Morris, R.M., R. C. Hannon, K. P. Helmond, D. G. Knock, H. W. Posamentier, 2000, Jurassic Alpine Sandstone, North Slope, Alaska: An example of shoreface deposition within a punctuated transgressive succession (abs.), AAPG Annual Meeting Abstract, New Orleans, Louisiana.

O'Connell, S., 2003, The unknown giants-low-permeability shallow gas reservoirs of southern Alberta and Saskatchewan, Canada (abs.): Canadian Society of Petroleum Geologists Convention Abstracts.

Pedersen, P.K., 2003, Stratigraphic relationship of Alderson (Milk River) strata between the Hatton and Abbey-Lacadena pools, southwestern Saskatchewan – preliminary observations: *in* Summary of Investigations 2003, v.1, Saskatchewan Geological Survey, Sask. Industry Resources, Misc. Rep. 2003-4.1, CD-ROM, Paper A-11, p.11.

Pemberton, S.G., M. K. Gingras, 2005, Classification and characterizations of biogenically enhanced permeability: AAPG Bulletin, vol. 89, 11, p.1493-1517.

Ratke, L., P. W. Voorhees,2002, Growth and coarsening: Ostwald ripening in material processing, Springer, pp. 117-118.

Robinson, C., S. Larter, and R. Spencer, 2008, Assessing shale gas potential of the Upper Colorado Group, southern Alberta: a multidisciplinary approach (abs.), 2008 CSPG, CSEG, and CWLS Convention Abstract, pp. 458-459.

Sayles, F.L., W. G. Deuser, J. E. Goudreau, W. H. Dickinson, T. D. Jickells, P. King, 1996, The benthic cycle of biogenic opal at the Bermuda Atlantic Time Series site: Deep-Sea Research, I, v. 43, p. 383–409.

Schmidt, V, and D. A. McDonald, 1979a, The role of secondary porosity in the course of sandstone diagenesis: In P.A. Scholle and P.R. Schluger, eds., Aspects of diagenesis: Society of Sedimentary Geology Special Publication 26, p. 175-208.

Schmidt, V., D A. McDonald, and R. L. Platt, 1977, Pore geometry and reservoir aspects of secondary porosity in sandstones: Bulletin of Canadian Petroleum Geology., v.25,p. 271-290.

Serra, O., 1984, Fundamentals of well-log interpretation: Elsevier Science Publishers B.V., p 7.

Stonecipher, S.A., 1999, Genetic characteristics of glauconite and siderite: implications for the origin of ambiguous isolated marine sand bodies: Society of Sedimentary Geology Special Publication 46, p191-204.

Surdam, R. C., S. W. Boese, and L. J. Crossey, 1984, In Clastic Diagenesis (eds McDonald, D. A., Surdam, R. C.): American Association of Petroleum Geologists, Tulsa, p. 127-150.

Tucker, M. E., 2001, Sedimentary Petrology: an introduction to sedimentary rocks. Blackwell Science, London, 3rd edition, p. 56.

van der Weijden, C.H., 2007, Silicon II: Marine Biogenic Silica: Integral Text. Department of Geosciences – Geochemistry Utrecht University, Utrecht The Netherlands, pp 1-52.

Wickenden, R.T.D., 1948, The Lower Cretaceous of the Lloydminster oil and gas area, Alberta-Saskatchewan: Geological. Survey of Canada., Paper 48-21.

Wilson, M. D., and E. D. Pittman, 1977, Authigenic clays in sandstones: recognition and influence on reservoir properties and paleoenvironmental analysis: Journal of Sedimentary Research, v.47, p.3 - 31.

Zhu, Q., A. C. Aller, F. Fan, 2006, Two-dimensional pH distributions and dynamics in bioturbated marine sediments: Geochimica et Cosmochemica Acta v.70, p. 4933-4949.

Zorn, M.E., S. V. Lalonde, M. K. Gingras, S. G. Pemberton, and K. O. Konhauser, K.O, 2006, Microscale oxygen distribution in various invertebrate burrow walls: Geobiology, v. 4, p 1-9.

Chapter 3: Biogenically Enhanced Permeability: A Petrographic Analysis of *Macaronichnus segregatus* in the Lower Cretaceous Bluesky Formation, Alberta, Canada.

3.1 Introduction

Petrography can be a useful technique in assessing reservoir quality in sediments; it presents informative views of mineralogical controls affecting reservoir quality, but is commonly overlooked due to the reliance on wireline log analysis and other large-scale reservoir evaluation methods such as numerical modeling. Petrography potentially provides a window into small-scale burrow-associated heterogeneities that influence the flow characteristics of hydrocarbon reservoir rocks. The Lower Cretaceous (Albian to Aptian) Bluesky Formation in the La Glace area of western Alberta, Canada represents a high-energy, upper shoreface succession that provides an excellent case study for the utility of petrographic analysis pertaining to biogenically enhanced reservoir quality because (1) the Bluesky Formation is a significant gas-bearing reservoir in the area; (2) there is locally good core control; and (3) burrow-associated enhanced permeability is evident. The La Glace field is located approximately 50 kilometers northwest of Grande Prairie, Alberta, Canada (Fig. 3.1).

The focus of this chapter is to present the results of petrographic techniques (thin section and scanning electron microscopy), along with conventional core analysis and minipermeametry data, in an attempt to explain the elevated permeability and associated reservoir quality of the

intensely bioturbated *Macaronichnus segregatus* zone of these upper shoreface sandstones that lies within the gas producing zone. Six cores were described in detail from the Bluesky Formation in the La Glace field, but to avoid repetition only one (100/06-24-074-07W6/00) will is presented below and discussed herein.

Biogenic alterations of reservoir flow and storage include a local increase of porosity and permeability. These can be due to reorganization of the sediment fabric associated with animal burrowing, or result from heterogeneous cement distribution influenced by the bioturbate texture. Biogenic enhancement of reservoir character may be especially important for play development in unconventional, thinly-bedded, silty to muddy, low permeability reservoirs that have been recently exploited in the United States and, in particular, western Canada where high-reserve and high-deliverability plays are nearing an end.

3.2 Study Area and Geological Setting

The study area is located in Township 074 and Range 07 west of the 6^{th} meridian in western Alberta, Canada (Fig. 3.1). Within the La Glace field, the Bluesky Formation produces from four pools with an initial established reserves of 1502 X $10^6 m^3$ (Walsh, 1999).

The Cretaceous (Aptian to Albian) Bullhead Group of the Western Canada Sedimentary Basin was deposited during a major episode of subsidence and sedimentation. The strata comprise mainly clastic rocks

derived from older strata as a result of a long period of uplift, exposure, and erosion (Mossop and Shetsen, 1994). The Lower Albian sediments were deposited during a regional southward transgression of the Moosebar Sea, and are stratigraphically complex and widely distributed (Brekke, 1995).

Figure 3.2 shows a stratigraphic chart with the north-west Plains terminology used in this study. The Lower Albian Bluesky Formation of the Bullhead Group is overlain conformably by the shales of the Wilrich Formation and underlain by the sandstones, shales, and coals of the Gething Formation. It correlates with the Glauconitic Formation of the Mannville Group of central Alberta, Canada and with the Wabiskaw Member of the Clearwater Formation of northern Alberta, Canada. The reservoir strata of the Bluesky Formation at La Glace has been interpreted by O'Connell (1997) as representing fluvial to estuarine deposits that overlie a lowstand unconformity which in turn is overlain by highstand shoreface deposits.

3.3 Previous Work

Clifton and Thompson (1978) first described *Macaronichnus segregatus* as a deposit feeding behavior of polychaete worms as they search for food in modern, high energy, well oxygenated, near shore sediments. They observed that these polychaetes ingest light-coloured minerals such as quartz and feldspar while avoiding dark-coloured mafic

minerals, leaving the burrow fill lighter in colour than the host sediment. Saunders (1989) recognized three distinct forms of *Macaronichnus* in the Upper Cretaceous Horseshoe Canyon Formation in Alberta, Canada, differentiated on the basis of foraging pathway configurations (1) *Macaronichnus simplicatus* characterized by random interpenetrating burrows; (2) *Macaronichnus segregatus* also characterized by random burrows, but show an avoidance of interpenetration structures; and (3) *Macaronichnus spiralis* characterized by distinct planispiral configurations. Pemberton et al., (2001) described the presence of *Macaronichnus segregatus* to be a diagnostic of the foreshore and upper shoreface depositional environment. Pemberton and Gingras (2005) demonstrated that permeability enhancement and vertical transmissivity can be enhanced in relatively low permeable sediments by bioturbation and the subsequent filling of burrows with contrasting sediment from overlying deposits. Pemberton and Gingras (2005) conclude that the grain segregation and passive sorting of *Macaronichnus segregatus* has led to elevated reservoir quality.

3.4 Methodology

Six Bluesky Formation cores were examined for this study in Twp. 074, Rge. 07W6 in the La Glace field (Fig. 3.1). All six cores showed elevated permeability within the *Macaronichnus* burrowed zone, but only one well (Talisman La Glace 100/06-24-074-07W6) was studied in

petrographic detail forming the central part of this paper. Figure 3.3 shows a schematic display of the core. Ten representative samples from the one-inch core plugs were chosen for standard format thin sections. Before preparation, the samples were impregnated with a blue-dyed epoxy resin to identify porosity and to preserve pore-filling material. The samples were stained with Alizarin Red S to differentiate calcite and dolomite, and with potassium ferricyanide to identify ferroan calcite and ferroan dolomite.

A detailed petrographic analysis was performed from the thin sections including a 200-point count per sample mineral inventory of framework and authigenic mineral phases (Table 3.1). The 95% confidence limit on the point count data for 200 counts is les than + or - 7%. This is considered an acceptable error for the purpose of this study, which is to show general mineralogical trends that may have an influence on reservoir quality.

Three hundred and twenty-eight spot permeability measurements were taken along the core's length at approximately 2 cm intervals using a mini probe permeameter to obtain data on permeability heterogeneity. A 7 x 12 measurement spot permeability grid was preformed using eighty-four spot permeability measurements over an area of core within the intensely bioturbated zone spaced approximately 1 cm apart. These data were mapped in an attempt to show the bioturbation behaviour of *Macaronichnus segregatus*.

Routine porosity and permeability core analyses were performed on thirty-two one-inch core plugs. Visual grain size measurements were taken on each of the thirty-two core plugs under a binocular microscope using a standard grain size chart (Table 3.2). No less than 100 long-axis grain-size measurements were also taken from each thin section using simple image analysis (Table 3.3).

Scanning electron microscopy and x-ray dispersive analysis were used to further refine mineral chemistry. Simple image analysis was used on an overview scan of a thin section representing *Macaronichnus* to segregate light and dark minerals into only two colours (black and white respectively) to better illustrate the unique behaviour of *Macaronichnus*.

3.5 Lithofacies, Petrology, and Reservoir Quality

The Bluesky Formation at La Glace can be divided into five distinct lithofacies based on lithology, sedimentary structures, ichnofossil assemblages, petrographic analysis, and reservoir quality. Figure 3.4 shows all point count data plotted on a Folk (2002) ternary diagram. Petrographically all samples taken from the 06-24-074-07W6 core are chert-rich litharenites and chert-pebble conglomerate. Figure 3.5 is a modified ternary diagram showing a distinction between lithofacies with best reservoir quality and poorest reservoir quality. Poor reservoir quality for this study was determined to be lees than 1 millidarcy of permeability. The rocks with the best reservoir quality have the highest chert content

while the rocks with the poorest reservoir quality have the highest ductile rock fragment content and carbonate cement.

It should be noted that there is a wide disparity between core analysis porosity and thin section point count porosity. This is due to microporosity in pore occluding kaolinite and microporous sedimentary rock fragments. This type of porosity (up to 6% in some samples) may be considered ineffective. Therefore, thin section point count porosity can be considered a good proxy for effective porosity.

3.5.1 Lithofacies 1: Interbedded sand and shale

This facies exhibits 1-3cm organic-rich shale interbedded with coarser-gained sandstones (Fig. 3.6). This lithofacies was not analyzed petrographically.

3.5.2 Lithofacies 2: Fine-grained, low-angle cross-stratified, carbonate cemented sandstone

Lithofacies 2 (Fig. 3.7a) consists of light grey, fine-grained sandstones with low angle cross stratification, interpreted to be hummocky cross-stratification, and internal scour surfaces. Trace fossils are rare and generally absent, but where present, they are representative of the *Skolithos* ichnofacies. Carbonate cement is pervasive throughout. This lithofacies is interpreted as high-energy storm deposits.

Petrographically this lithofacies is a well-sorted, subangular to subrounded, mid- to upper fine-grained litharenite (Fig. 3.7b). The

framework minerals are dominated by monocrystalline quartz (20% avg.) and chert (10% avg. light coloured and 7% avg. dark coloured). Sedimentary rock fragments (24% avg.) are mainly detrital carbonate fragments and minor illitic shale clasts. Polycrystalline quartz (6% avg.), volcanic rock fragments (2% avg.), and metamorphic rock fragments (3% avg.) make up the remainder of the detrital clasts. The authigenic minerals are dominated by ferroan carbonate cement (19% avg.). Silica cement (2% avg.) occurs as syntaxial overgrowths on monocrystalline quartz grains, kaolinite (5% avg.) likely the result of feldspar degradation, and pyrite (1% avg.) is also present.

Reservoir quality of the lithofacies is poor owing to pervasive ferroan carbonate cement (Fig. 3.7b). Core porosities range from 4 to 11%, but poor pore connectivity is evident from poor permeability values of 0.01 and 0.57 millidarcies. Spot permeametry measurements show localized permeability up to 1 millidarcy.

3.5.3 Lithofacies 3: Pebbly sandstone to localized matrix-supported conglomerate

Lithofacies 3 (Fig. 3.8a) consists of dark grey, upper fine to mid-medium grained chert-rich sandstone and chert pebble matrix-supported conglomerate. These beds are generally thin (10-20 cm) and are separated by fining-upward sands and shales.

Petrographically Lithofacies 3 is a moderately well sorted, but locally poorly sorted, dominantly mid-medium grained, pebbly litharenite to localized matrix-supported chert-pebble conglomerate (Fig. 3.8b). Chert (37% avg. light coloured and 18% avg. dark coloured) dominates the framework grains. Monocrystalline quartz (11% avg.) is also present. Polycrystalline quartz (4% avg.), sedimentary rock fragments (4% avg.), volcanic rock fragments (2% avg.), and metamorphic rock fragments (2% avg.) make up the remainder of the detrital clasts. The authigenic minerals include ferroan carbonate cement (6% avg.), silica cement (1% avg.), kaolinite (6% avg.), and pyrite (1% avg.).

Reservoir quality of this lithofacies is excellent (Fig. 8b). Core porosity is 14% and permeability is 199 mD. However, this zone was not the primary target of oil and gas companies as it is, in general, very thin and may be water wet.

3.5.4 Lithofacies 4a: Fine to medium-grained low-angle cross-stratified sandstone

Lithofacies 4a (Fig. 3.9a) includes dark grey, upper fine- to medium-grained, chert-rich sandstones that are in sharp contact with the overlying glauconitic sands and sideritic shales of the Wilrich Formation. Low angle cross stratification is abundant. Rare small-scale trough cross beds occur at the top of this unit. Rare internal scour structures are also present. Thin organic-rich shales lie near the base. Carbonate cement is present, but pervasive near the base. Localized *Macaronichnus* burrows

are present, suggesting deposition in a shallow, high-energy shoreface environment.

Petrographically this lithofacies is a moderately well to well sorted, upper fine to mid-medium grained, subangular to subrounded litharenite (Fig. 3.9b and 3.9c). Chert (16% avg. light coloured and 13% avg. dark coloured) and monocrystalline quartz (11% avg.) dominate the framework grains. Sedimentary rock fragments (15% avg.), polycrystalline quartz (8% avg.), volcanic rock fragments (3% avg.), metamorphic rock fragments (3% avg.), and plagioclase feldspar (1% avg.) represent the remainder of the detrital clasts. One sample at 1567.0m contains 10% pseudomatrix resulting from the mechanical compaction of illitic and micaceous shale clasts into adjacent pore space. The authigenic minerals include localized ferroan carbonate cement (11% avg.), silica cement (3% avg.), kaolinite (5% avg.), and pyrite (1% avg.).

Reservoir quality is marginal (Fig. 3.9b and 3.9c). The average porosity is 10% and permeabilities range from 0.01 to 2.36 mD. Average point count porosity from the thin sections is 4%. This suggests that approximately half of the measured core analysis porosity is due to microporosity attributed to microporous kaolinite and partially leached unstable clasts. Localized pervasive ferroan carbonate cement completely occludes porosity and associated reservoir quality. This lithofacies is considered the reservoir facies.

3.5.5 Lithofacies 4b: Fine to mid-medium grained intensely bioturbated sandstone

Lithofacies 4b is approximately 1 meter in thickness and lies within Lithofacies 4a (Fig. 3.10). This lithofacies is similar to and is in sharp contact with the Lithofacies 4a, however the entire zone is intensely burrowed with *Macaronichnus segregatus* defined by tabular, non-branching burrows that have a distinct dark-coloured grain halo that is lithologically different from the light-coloured burrow fill and surrounding matrix. Burrows are approximately 1-2 mm in diameter. The unit appears homogenized and all bedding features have been obliterated by burrowing activities except for rare, poorly defined low-angle laminations. Although lithologically and texturally similar to Lithofacies 4a, Lithofacies 4b (Fig. 3.10b) has a higher chert content, lower monocrystalline quartz content, and is dominantly upper fine to medium grained. However, pervasive biogenic reworking of this sand is evident. The grains are not randomly distributed as in Lithofacies 4a and a halo of dark-coloured grains consisting of chert, shale clasts, and organic matter surround the light coloured burrow-fill consisting of monocrystalline quartz, chert, and minor feldspar (Fig. 3.10c).

Reservoir quality of this lithofacies is elevated with a core porosity value of 13% and a permeability of 8.43 mD. Lithofacies 4a and 4b are consistently perforated on wireline logs and are the main target of oil and

gas companies in the Bluesky Formation at La Glace. The permeability enhancement of Lithofacies 4b is scrutinized below

3.6 *Macaronichnus segregatus* and Reservoir Quality

Figure 3.11 shows spot permeability measurements by lithofacies. These data show that there is very little permeability variation in the *Macaronichnus* burrowed facies. The permeability in this lithofacies ranges 1-10 millidarcies. There is a greater range of permeability in Lithofacies 4a. While some permeability measurements are above 1 millidarcy in Lithofacies 4a, most permeability measurements fall well below. Lithofacies 3 shows the best permeability, but is not a reservoir target as mentioned above. Some permeability measurements are up to 1 millidarcy in Lithofacies 2, but these data points are highly localized and poorly developed within the lithofacies.

Figure 3.12 shows a maximum permeability versus porosity plot of measured core analysis data. These data show that the *Macaronichnus* burrowed Lithofacies 4b lies on a different trend from Lithofacies 4a. These data extrapolated to 15% porosity would yield permeabilities of approximately 4 millidarcies for Lithofacies 4a and approximately 20 millidarcies for Lithofacies 4b.

Figure 3.13 shows visual grain size estimates of all 32 core plugs versus maximum measured permeability. These data show that almost all of the samples in the bioturbated zone of Lithofacies 4b have higher

permeability than samples with the same grain size in the non-bioturbated zone of Lithofacies 4a. All of the average visual grain size measurements taken from the core plugs are slightly lower than the average grain sizes measured on the thin sections by image analysis. The grain size data from image analysis on the thin sections show Lithofacies 4b to have an average grain size of 1.57 phi (mid-medium grained) while the average grain size measured visually from the plugs is 2.00 phi (upper fine to lower medium grained). This is likely due to the scale at which each type of measurement was taken. Thin section grain size analysis was done on one photomicrograph at 100x magnification and the visual grain size estimates were done directly on the core plug end at 20x magnification. The visual grain size measurements cover a greater area than the thin section measurements therefore the visual measurements likely show a better representation of the actual grain size.

Spot permeability measurements across a portion of the intensely *Macaronichnus* burrowed zone was preformed in a 7 X 12 measurement grid pattern (Fig. 3.14a). A graphical representation, or permeability map, of this spot permeametry data is shown in Figure 3.14b. This map indicates *Macaronichnus segregatus* burrows have effectively increased isotropy of the permeability of this zone by the almost complete obliteration of muddy laminations that can act as permeability barriers as in Lithofacies 4a. Permeability is increased towards the base of the sample.

Figure 3.15a shows an overview scan of a large format thin section taken over the *Macaronichnus* burrowed zone (Lithofacies 4b). Figure 3.15b is the same field of view, but with dark-coloured rock fragments shown in black only. Light-coloured fragments remain white showing the burrow fill. This image clearly shows that the *Macaronichnus segregatus* burrows are visually defined by a halo of dark-colored rock fragments. The burrows can be seen in cross-section and longitudinally and are oriented horizontally to subhorizontally.

This unique behavior has been reported by other workers (e.g., Clifton and Thompson, 1978; Pemberton et al., 2001; Gingras et al., 2002; and Gingras et al., 2007). Dafoe et al., (2008) recently showed that the modern polychaete, *Euzonus mucronata*, preferentially ingests felsic grains over mafic and en masse feeding in felsic-rich deposits provides a mechanism for ancient *Macaronichnus segregatus*. Pemberton et al., (2001) suggest that the same modern polychaete *Euzonus mucronata* ingests sand in search for an epigranular bacterial food source and excretes the ingested sand that backfills the burrow structure. Clifton and Thompson (1978) originally described *Macaronichnus segregatus* and found the modern polychaete *Ophelia limicina* to exhibit identical behavior. In all of these examples, the polychaetes burrow structure contains light-colored grains as the fill and dark-colored grains as a burrow mantle.

It is apparent in the Bluesky Formation that presence of *Macaronichnus* burrows in the chert-rich sediment of Lithofacies 4b is key

to reservoir preservation. Chert, like quartz, resists the effects of mechanical compaction, thereby preserving primary porosity, much better than ductile detrital grains (i.e. shale clasts), which under the stress of depositional overburden, can be squeezed into adjacent pore space; a process that severely reduces reservoir quality. Moreover, pore-occluding authigenic syntaxial quartz overgrowths that form on monocrystalline quartz grains do not form on chert grains owing to the microcrystalline structure of chert. Alternatively, euhedral quartz microcrystals can form on chert fragments and can cause porosity reduction, but this rarely results in complete porosity occlusion. Landers et al., (2008) have shown by using simulated quartz cementation models that quartz cementation rates are significantly slower for polycrystalline quartz and chert. Larese and Hall (2003) noted that chert-rich sandstones may have better reservoir quality than similar intervals with greater amounts of monocrystalline quartz.

The dark-coloured detritus forming the burrow mantle includes chert, shale clasts, and organic-rich grains. Energy dispersive x-ray analysis (EDX) showed the dark- colored chert in the Bluesky Formation to have high iron content (Fig. 3.16). The elevated iron content may be attributed to the presence of authigenic pyrite and/or hematite that formed in the parent sediment. In-situ secondary iron precipitation localized to the burrow mantle can be ruled out as the dark iron-rich fragments appear in

the non-bioturbated sand indicating that the iron-rich grains were transported.

The result of grain-segregation into the burrow fills is that zones with a chert-rich lithology are re-sorted locally. The ancient burrowers of the Bluesky Formation have conveniently rearranged the sediment locally leaving light-coloured compaction and cement-resistant chert and quartz as the burrow fill while discarding dark-coloured compactable clasts (shale and organic grains) to the burrow mantle setting up permeability conduits within this sediment. The dark-coloured chert fragments behave similarly as the light-coloured chert fragments, but are in general part of the burrow mantle. In some burrows where quartz grains alone make up the burrow fill, syntaxial quartz overgrowths have formed and primary porosity is correspondingly reduced. This indicates that if the Bluesky detritus of Lithofacies 4b had a higher quartz to chert ratio or if quartz and chert were evenly distributed, the reservoir quality would be severely reduced due to silica cementation of the primary porosity.

3.7 Conclusion

The Bluesky Formation in the La Glace area in western Alberta, Canada is an upper shoreface deposit comprising fine to medium-grained lithic sandstones with thin conglomeratic lag deposits and fine grained carbonate cemented storm beds. Within the lithic reservoir sand is a medium-grained litharenite interval heavily bioturbated with

Macaronichnus segregatus. This bioturbated zone is indicative of high-energy shoreface deposits, shows an elevated preserved permeability than in the surrounding sediment.

Petrographic techniques have aided in understanding the effects *Macaronichnus segregatus* has on reservoir quality in these upper shoreface sediments. Utilization of thin sections and scanning electron microscopy has led to the interpretation that the tracemaker of *Macaronichnus segregatus* avoided iron-rich detrital fragments while exploiting the sediment for food. This grain avoidance led to a re-sorting of the sand that shed the dark-coloured rock fragments to outline the burrow while light-coloured competent grains were ingested and became the burrow fill. The light-coloured burrow fill contains a high chert to quartz ratio. Primary reservoir quality can be preserved in the presence of chert as pore-occluding quartz overgrowths do no form on chert fragments as they do on monocrystalline quartz, thus leaving open, well connected primary pores and hence elevated permeability. Chert fragments are resistant to the effects of mechanical compaction and are not easily squeezed into adjacent pore space as are ductile rock fragments.

Detailed petrographic examination of micro-fabrics is essential to assessing reservoir quality in burrowed hydrocarbon-bearing sediments leading to a better understanding of the depositional environments that contain *Macaronichnus* and similar burrowed sediment. Important also is the recognition that hydrocarbon production from bioturbated rock is

generally more complex than production from laminated media. This is because flow paths through burrow-related flow conduits are comparatively tortuous. Further complicating geological and reservoir models, these tortuous, heterogeneous media present notable complications for reservoir development. Burrows may provide flow conduits that interact extensively with the surrounding matrix as shown in this study; their tortuous nature implies that dead ends and cut-offs may be common. An understanding of how burrow-associated heterogeneities control fluid flow within sedimentary units is necessary if production from bioturbated reservoirs is to be optimized.

Depth	Texture				Framework Grains (%)									Authigenic Minerals (%)				Matrix (%)	Reservoir		
Meters (m)	Mean Framework Grain Size From Thin Section Image Analysis (Phi)	Mean Framework Grain Size From Visual Estimation (Phi)	Sorting (Standard Deviation of Phi)	Sorting	Monocrystalline Quartz	Polycrystalline Quartz	Feldspar	Light-Coloured Chert	Dark-Coloured Chert	Sedimentary Rock Fragments	Volcanic Rock Fragments	Metamorphic Rock Fragments	Glauconite + Altered Glauc:	Silica Cement	Ferroan Carbonate Cement	Kaolinite	Pyrite	Pseudomatrix	Core Analysis Porosity (%)	Core Analysis Permeability (mD)	Thin Section Point Count Porosity (%)
Lithofacies 4a: Fine-medium grained low-angle cross-stratified sandstone																					
SP 2 1565.85	1.94	2.30	0.59	MS	23.0	4.0	0.5	18.5	20.0	15.0	0.5	2.5	tr	3.5	0.5	5.5	0.0	0.0	11.90	1.39	6.5
SP 3 1566.05	1.93	2.30	0.53	MWS	22.5	9.5	0.5	19.0	19.5	9.5	1.5	2.5	tr	3.5	0.0	6.5	1.0	0.0	14.00	2.36	4.5
SP 8 1567.00	2.16	2.30	0.41	WS	23.5	10.0	3.5	14.5	6.0	18.5	2.5	2.0	tr	5.0	0.0	3.0	1.0	10.0	10.00	0.22	1.5
SP 13 1568.22	2.11	2.30	0.48	WS	20.5	6.0	0.0	12.5	12.5	2.5	10.0	2.0	tr	1.0	28.0	3.5	1.0	0.0	5.40	0.01	0.5
SP 16 1568.92	1.77	2.00	0.44	WS	20.5	9.5	0.0	14.5	10.0	16.5	3.5	4.5	tr	2.5	5.5	4.0	2.5	0.0	11.10	1.68	6.5
SP 20 1569.82	2.36	2.50	0.36	WS	19.0	9.0	0.0	15.5	11.0	28.0	2.5	2.0	tr	2.0	5.0	0.0	3.0	0.0	8.50	0.21	3.0
Lithofacies 4b: Fine- medium grained intensely bioturbated sandstone																					
SP 10 1567.5	1.57	2.00	0.37	WS	17.0	10.0	0.0	20.0	22.5	7.0	2.5	2.0	tr	3.5	0.0	5.0	1.0	0.0	13.10	8.43	9.5
Lithofacies 3: Pebbly sandstone to localized matrix supported conglomerate																					
SP 28 1572.45	1.51	2.80	0.66	MWS	10.5	4.0	0.0	36.5	18.0	4.0	1.5	1.5	tr	1.0	5.5	5.5	0.5	0.0	14.00	199.00	11.5
Lithofacies 2: Fine-grained, low-angle cross-stratified, carbonate cemented sandstone																					
SP 29 1572.82	2.24	2.80	0.39	WS	20.0	5.0	0.0	10.0	8.0	17.0	2.0	2.5	tr	1.0	28.0	5.0	0.5	0.0	4.20	0.01	1.0
SP 31 1574.58	2.75	2.80	0.32	WS	19.0	6.0	0.0	10.0	6.0	30.0	2.5	3.0	tr	2.5	9.0	5.0	1.0	0.0	11.30	0.57	6.0

ABBREVIATIONS

PS = Poorly Sorted
MS = Moderately Sorted
MWS = Moderately Well Sorted
WS = Well Sorted

MF = Mid-Fine Grained
UF = Upper Fine Grained
LM = Lower Medium Grained
MM = Mid-Medium Grained

SP = Small Plug

Table 3.1 Thin section point count and grain size data.

Sample	Range (Phi)		Avg (Phi)	Facies
SP1	3.30	1.80	2.30	4a
SP2	3.30	0.80	2.30	4a
SP3	3.30	2.30	2.30	4a
SP4	3.30	1.80	2.30	4a
SP5	3.30	1.80	1.80	4a
SP6	3.30	0.80	2.50	4a
SP7	3.30	1.80	2.30	4a
SP8	3.80	1.80	2.30	4a
SP9	3.80	0.50	2.00	4b
SP10	3.80	0.50	2.00	4b
SP11	3.30	2.50	2.30	4b
SP12	3.30	1.30	2.30	4b
SP13	3.30	1.50	2.30	4a
SP14	3.30	1.30	2.00	4a
SP15	3.30	1.30	2.00	4a
SP16	3.30	1.50	2.00	4a
SP17	3.30	1.50	2.00	4a
SP18	3.30	1.80	2.30	4a
SP19	3.30	1.80	2.30	4a
SP20	3.30	1.30	2.50	4a
SP21	3.30	1.80	2.30	4a
SP22	3.30	1.80	2.30	4a
SP23	3.30	1.80	2.30	4a
SP24	3.30	1.80	2.30	4a
SP25	2.80	0.80	1.50	4a
SP26	2.80	-1.80	1.00	3
SP27	3.30	1.30	2.00	3
SP28	3.30	-3.80	1.50	3
SP29	3.30	1.50	2.80	3
SP30	3.30	1.50	2.80	2
SP31	3.30	1.50	2.80	2
SP32	3.30	1.50	2.80	2

Table 3.2 Visual grain size estimates from core plugs. Note grain size average is visual not statistical.

Sample	Range (Phi)		Avg (Phi)	Facies
SP2	3.17	0.61	1.94	4a
SP3	3.20	0.38	1.93	4a
SP8	3.25	1.08	2.16	4a
SP10	2.43	0.57	1.57	4b
SP13	3.75	0.91	2.11	4a
SP16	2.97	0.46	1.77	4a
SP20	3.48	0.96	2.36	4a
SP28	2.95	-0.55	1.51	3
SP29	3.21	1.36	2.24	2
SP31	3.51	1.96	2.75	2

Table 3.3 Image analysis grain size measurements from thin sections

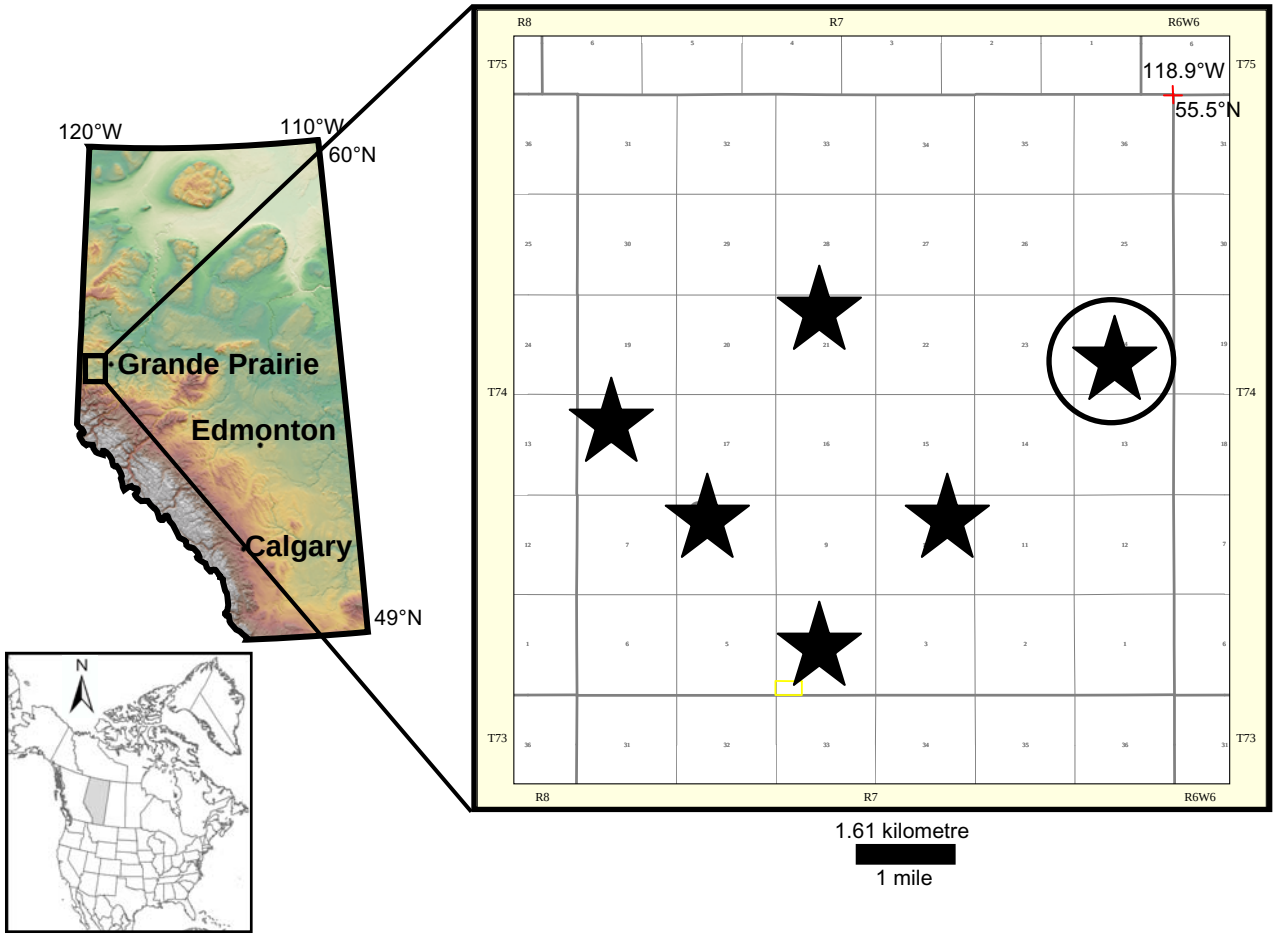

Figure 3.1 Study area map. Box indicates the La Glace area. Stars indicate cored wells viewed. Circle shows location of 06-24-074-07W6 that was described in detail for this study.

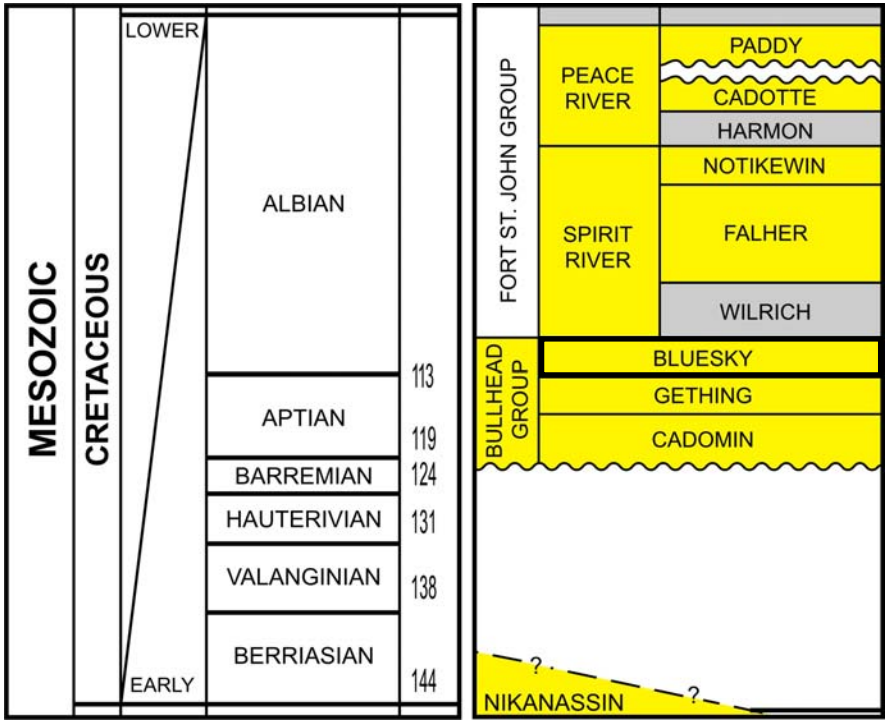

Figure 3.2 Geological time scale showing stratigraphic nomenclature for the La Glace area. The Bluesky Formation is highlighted by black box.

Well Name: Talisman et al La Glace 06-24-074-07W6

Formation: Bluesky

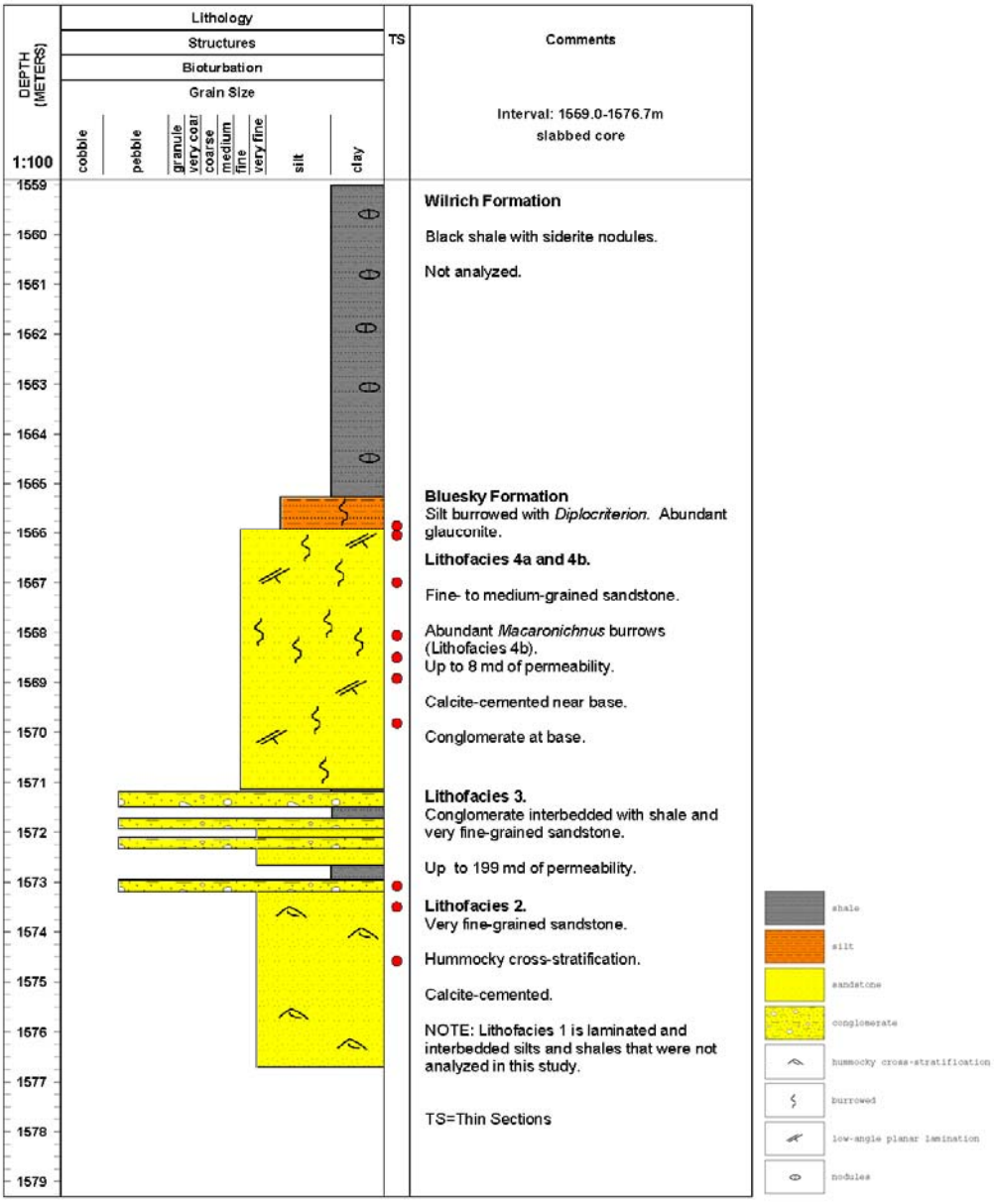

Figure 3.3 Core description for 100/06-24-074-07W6/00

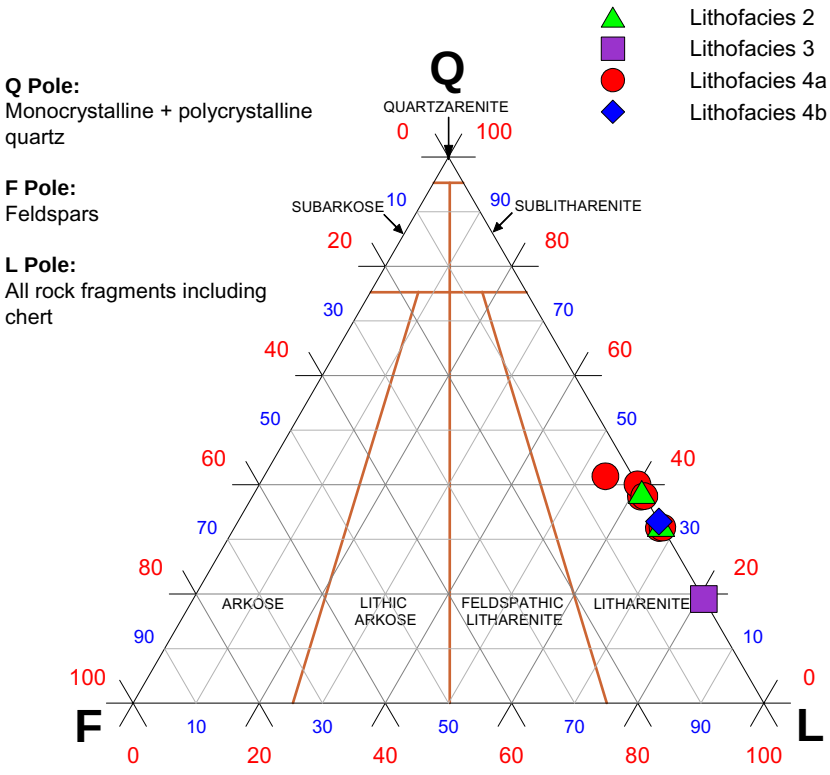

Figure 3.4 Folk (2002) ternary plot showing petrographic data.

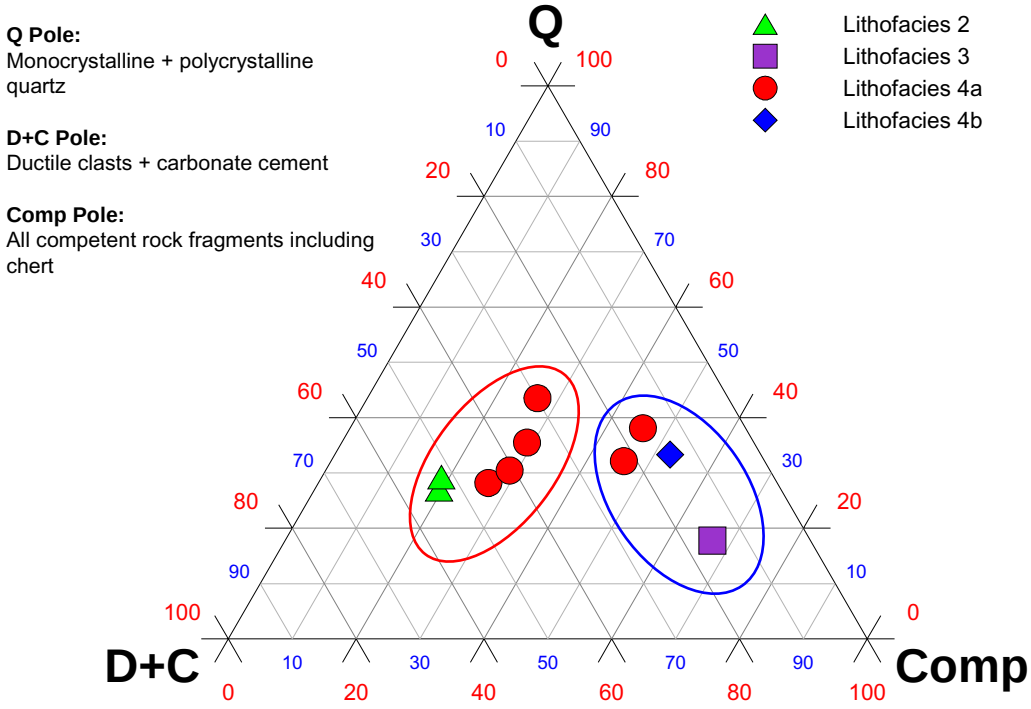

Figure 3.5 Modified ternary plot with quartz (Q), competent clasts (Comp) and ductile and carbonate cement (D+C) as end members. This plot shows the distinction between reservoir (circle on the right) and non-reservoir rocks (circle on the left). A 1 millidarcy cut-off was used in this study to define reservoir versus non-reservoir rock.

Figure 3.6 Lithofacies 1: Interbedded sand and shale.
This facies exhibits 1-3cm organic-rich shale interbedded with coarser-gained sandstones and was not analyzed petrographically (scale is 10cm long).

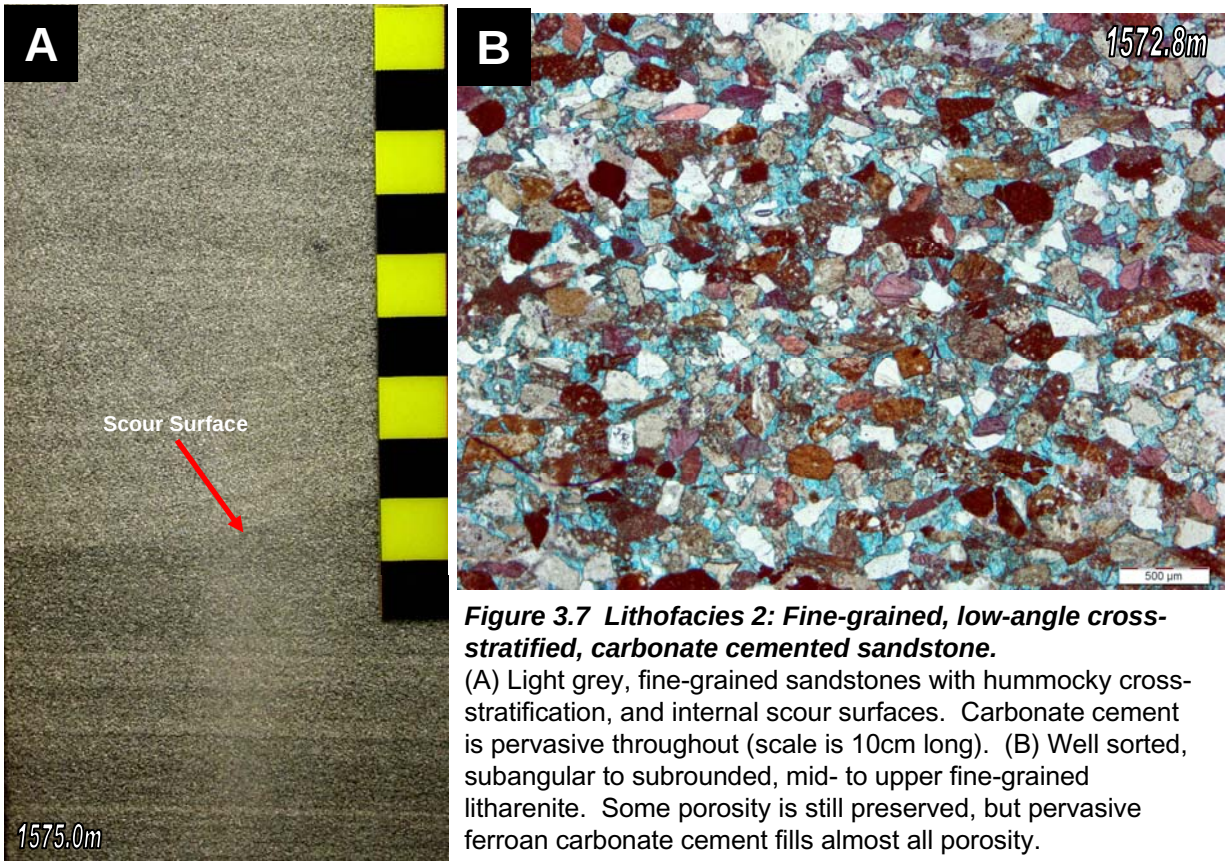

Figure 3.7 Lithofacies 2: Fine-grained, low-angle cross-stratified, carbonate cemented sandstone.
(A) Light grey, fine-grained sandstones with hummocky cross-stratification, and internal scour surfaces. Carbonate cement is pervasive throughout (scale is 10cm long). (B) Well sorted, subangular to subrounded, mid- to upper fine-grained litharenite. Some porosity is still preserved, but pervasive ferroan carbonate cement fills almost all porosity.

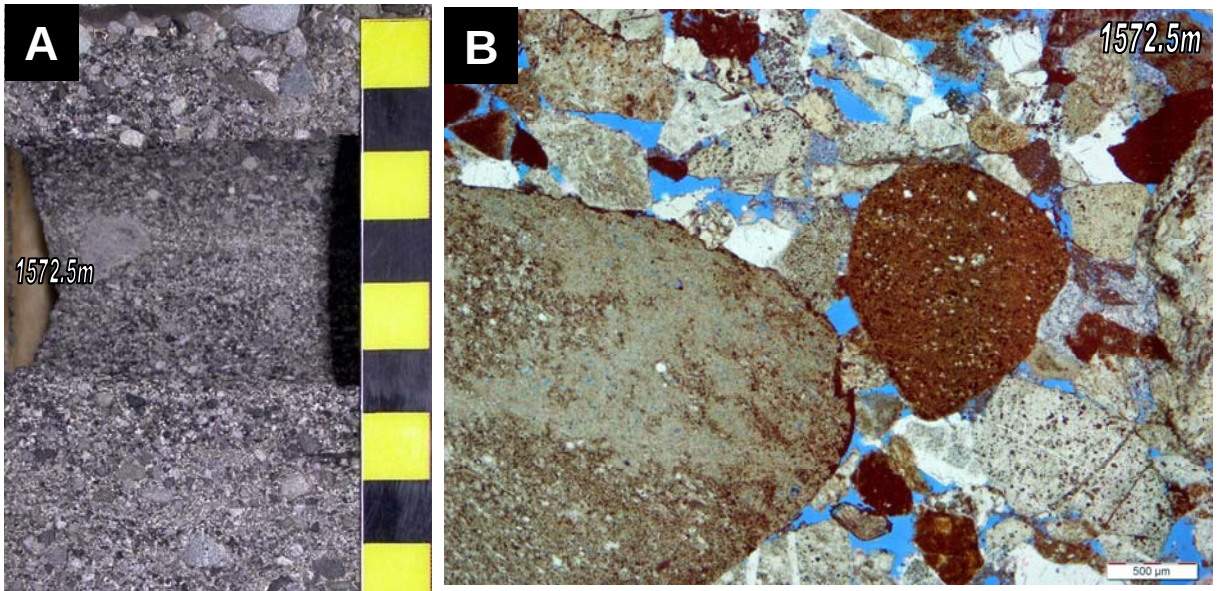

Figure 3.8 Lithofacies 3: Pebbly sandstone to localized matrix-supported conglomerate.
(A) Dark grey, upper fine to mid-medium grained chert-rich sandstone and chert-pebble matrix supported conglomerate. These beds are generally thin (10-20 cm) and are separated by fining-upward sands and shales (scale is 10cm long). (B) Moderately well sorted, but locally poorly sorted, dominantly mid-medium-grained, pebbly litharenite to localized matrix-supported chert-pebble conglomerate. Porosity preservation is excellent.

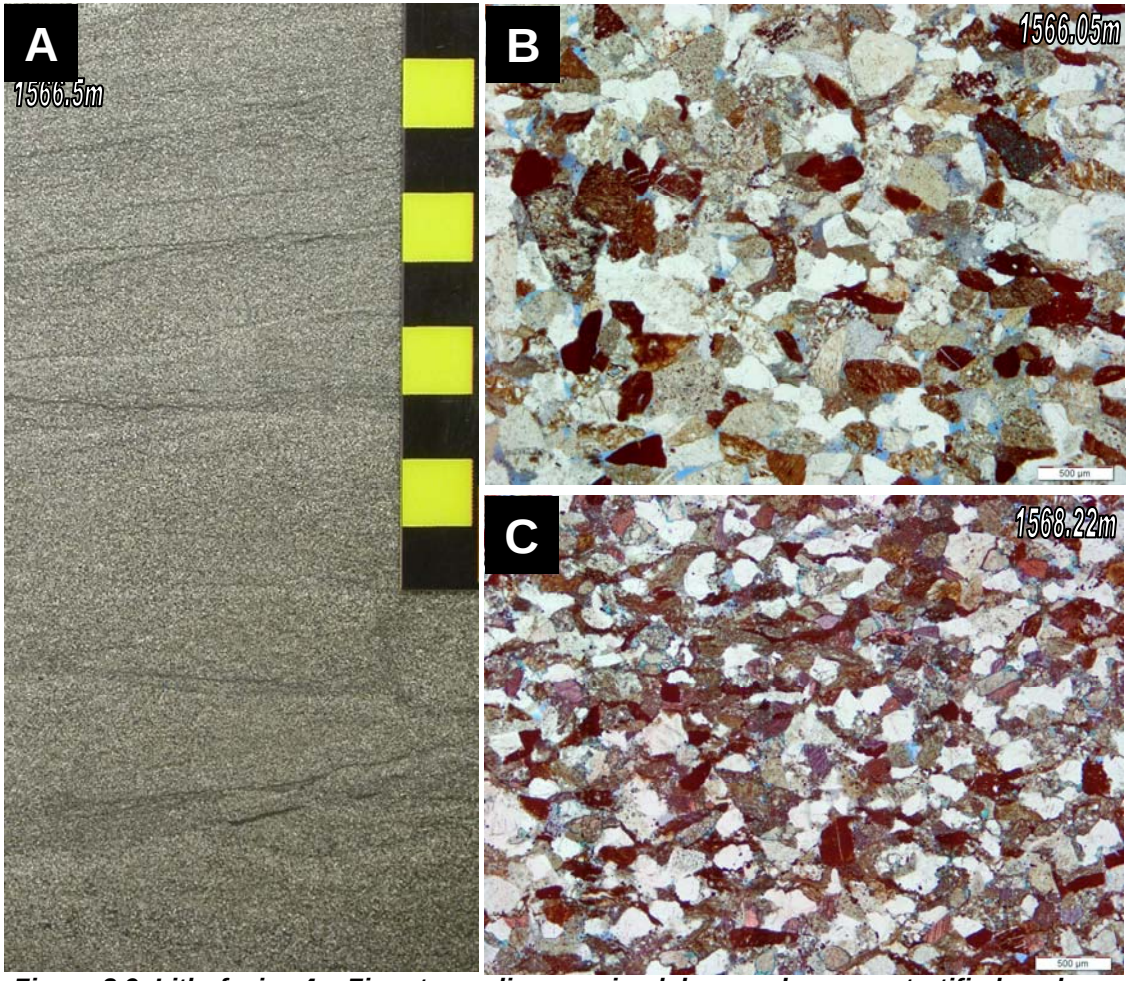

Figure 3.9 Lithofacies 4a: Fine- to medium- grained, low-angle cross-stratified, and locally bioturbated sandstone. (A) Dark grey, upper fine- to lower medium-grained, chert-rich sandstones with low angle cross stratification. Rare small-scale trough cross beds occur at the top of this unit. Rare internal scour structures are also present. Carbonate cement is present, but pervasive near the base. Minor *Macaronichnus* burrows are present (scale is 9 cm long). (B) Moderately well to well sorted, upper fine to lower medium grained, subangular to subrounded litharenite. (C) Finer grained than above and carbonate cemented (this sample was taken near the base of the unit).

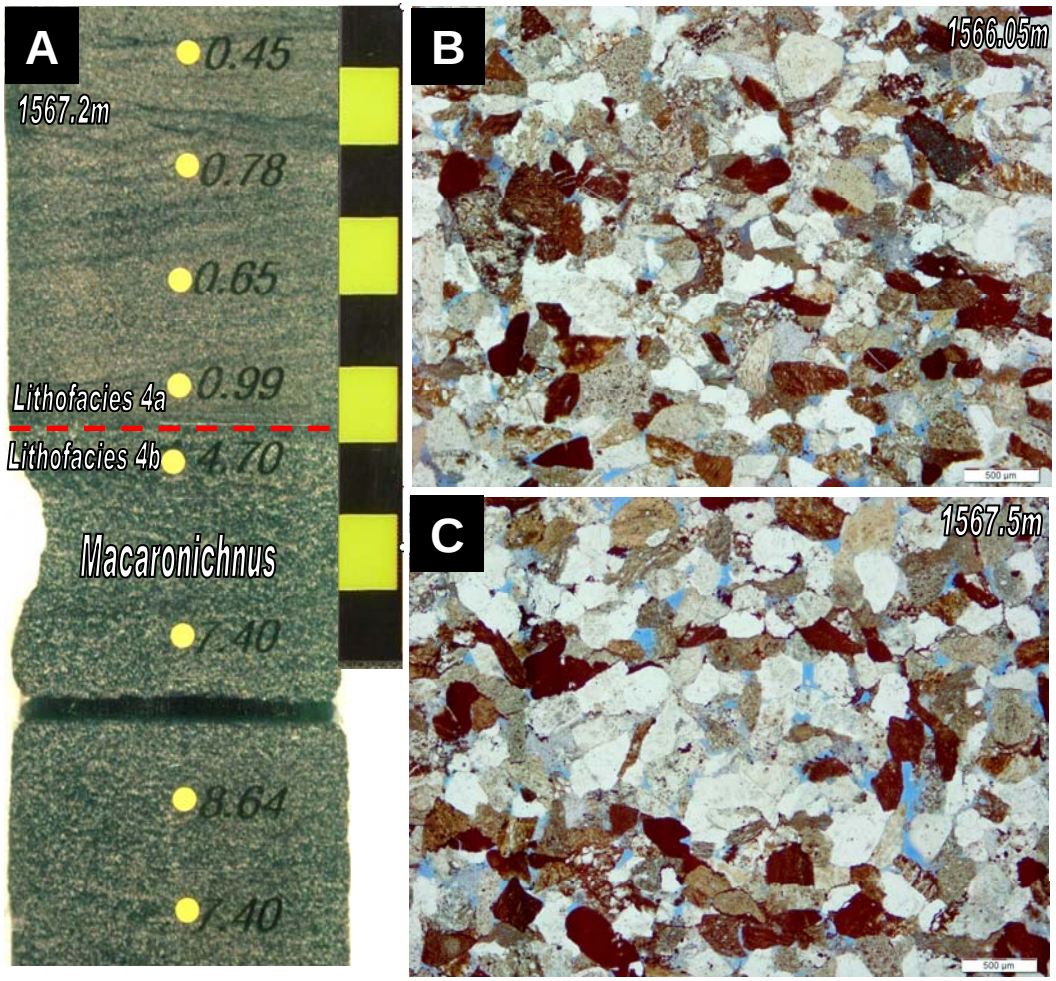

Figure 3.10 Lithofacies 4b: Fine- to mid-medium grained intensely bioturbated sandstone.

(A) Sharp contact between Lithofacies 4a and 4b which is completely burrowed with *Macaronichnus*. Note the elevated profile permeability measurements across the contact (scale is 9cm long and permeability is in millidarcies). Permeability increases by an order of magnitude across the contact. (B) This photomicrograph shows chaotic sorting of light and dark-coloured grains. (C) This photomicrograph shows a *Macaronichnus* burrow with dark grains forming the halo and light-coloured quartz and chert as the burrow-filling.

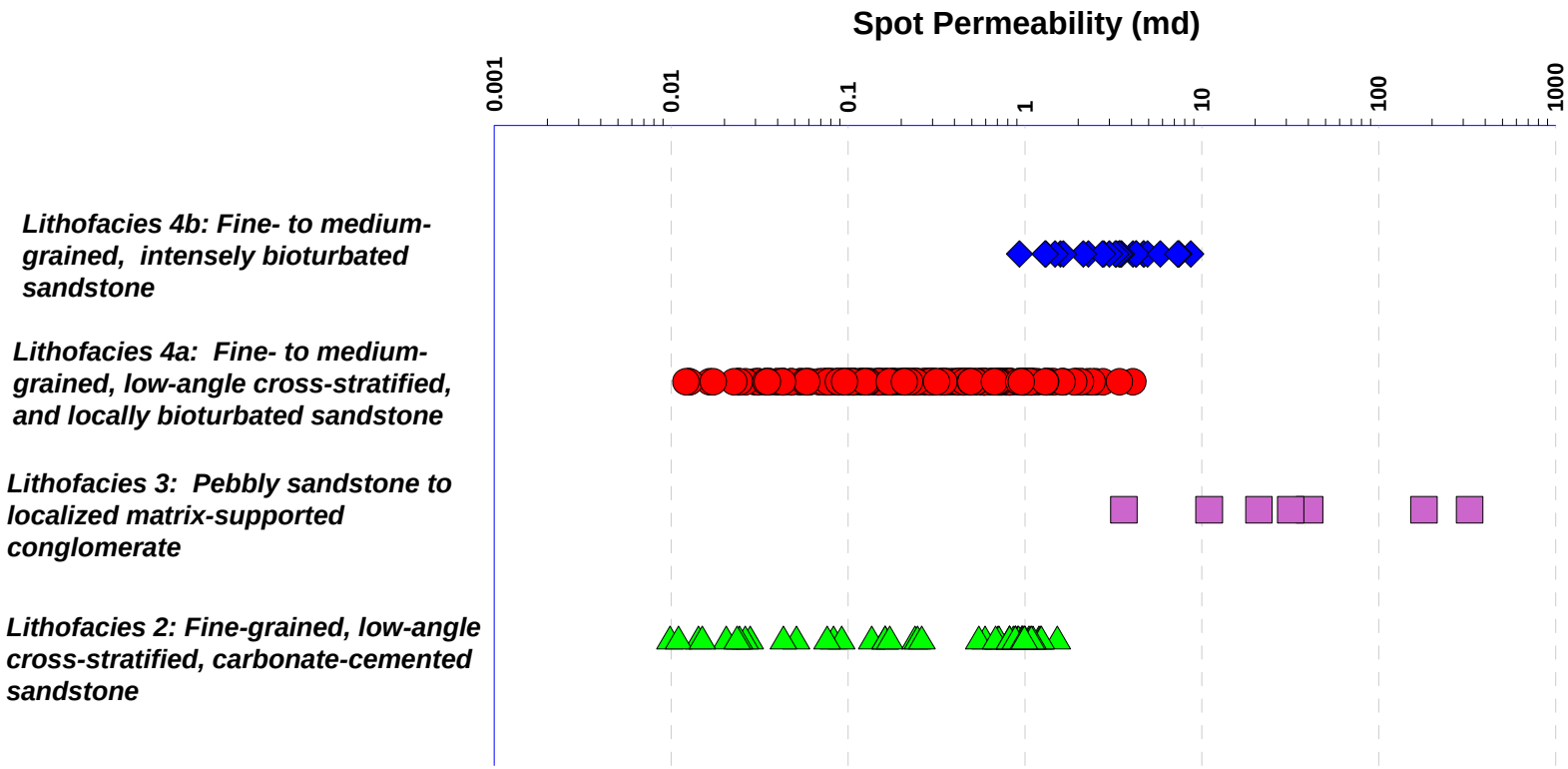

Figure 3.11 Spot permeability measurements by lithofacies. These data show that there is very little permeability variation in the *Macaronichnus* burrowed facies. The permeability in this lithofacies ranges 1-10 millidarcies. There is a greater range of permeability in Lithofacies 4a. While some permeability measurements are above 1 millidarcy in Lithofacies 4a, most permeability measurements fall well below. Lithofacies 3 shows the best permeability, but is not a reservoir target as mentioned. Some permeability measurements are up to 1 millidarcy in Lithofacies 2, but these data points are highly localized and poorly developed within the lithofacies.

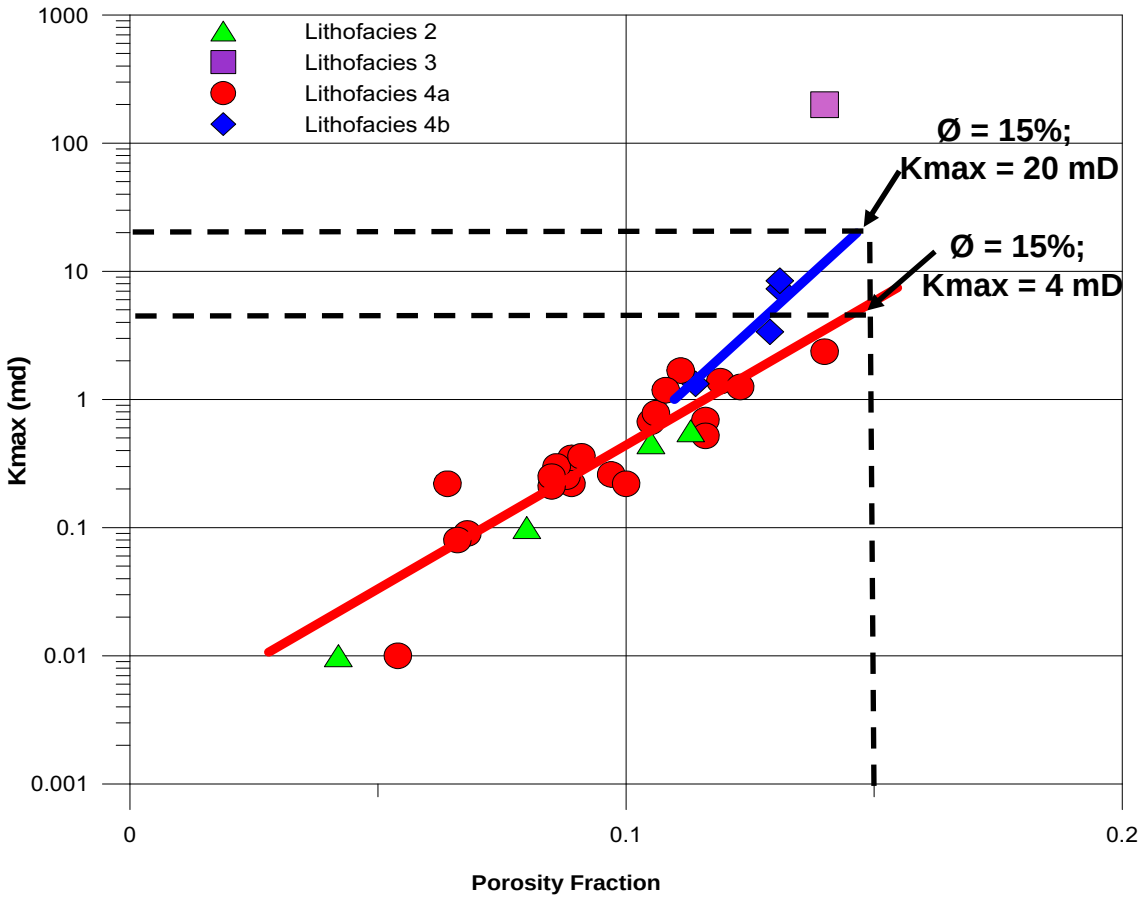

Figure 3.12 Maximum permeability versus porosity plot of measured core analysis data. These data show that the *Macaronichnus* burrowed Lithofacies 4b lies on a different trend from Lithofacies 4a. These data extrapolated to 15% porosity would yield permeabilities of approximately 4 millidarcies for Lithofacies 4a and approximately 20 millidarcies for Lithofacies 4b.

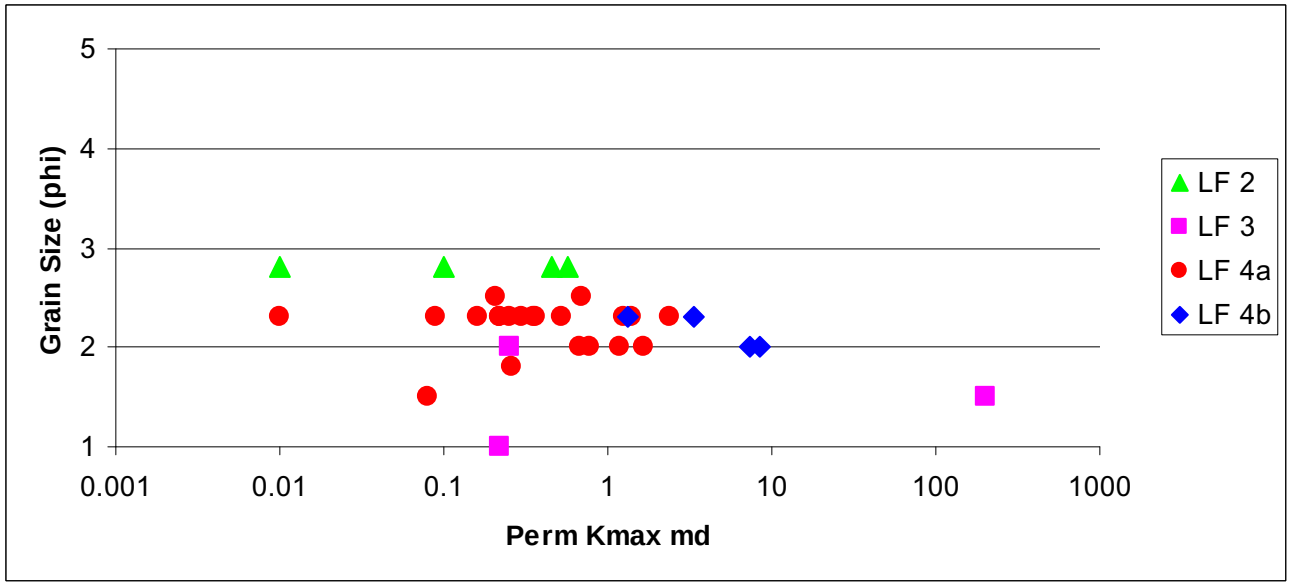

Figure 3.13 Visual grain size estimates of all 32 core plugs versus maximum measured permeability. These data show that almost all of the samples in the bioturbated zone of Lithofacies 4b have higher permeability than samples with the same grain size in the non-bioturbated zone of Lithofacies 4a.

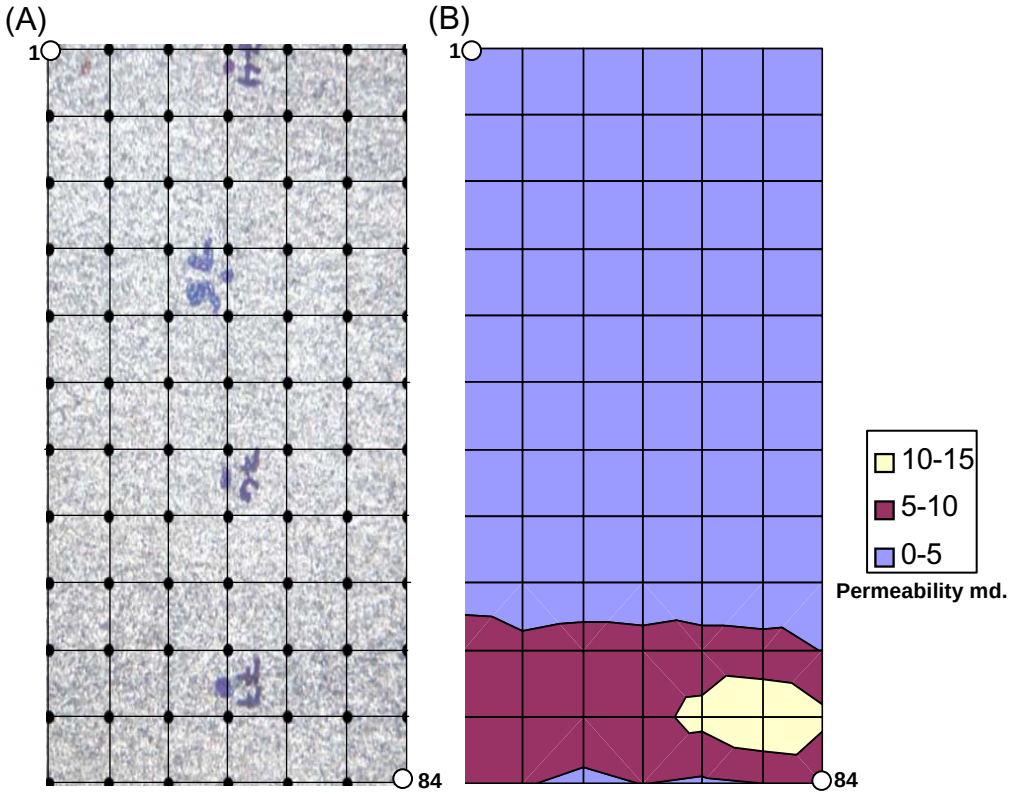

Figure 3.14 (A) Spot permeability measurements across a portion of the slabbed core in the intensely *Macaronichnus* burrowed zone in a 7 X 12 (points 1 and 84 are marked for reference) measurement grid pattern. (B) A graphical representation, or permeability map, of this spot permeametry data. This map indicates *Macaronichnus segregatus* burrows have effectively increased the isotropy of the permeability of this zone. Permeability is increased towards the base of the sample. Numbers on core in photo (A) are from whole core mini permeametry measurements. Scale bar is 1 cm.

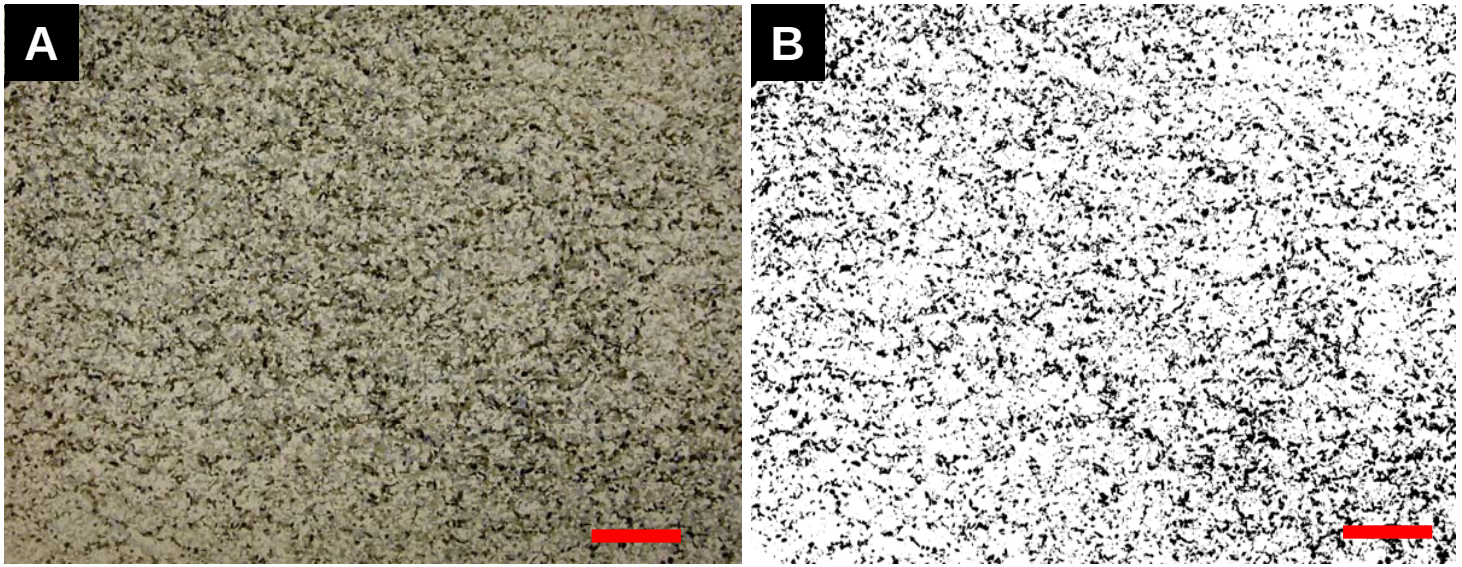

Figure 3.15 (A) Overview photo of *Macaronichnus* burrowed sand of Lithofacies 4b. (B) The same field of view showing image enhanced burrow structures. The burrow halo is outlined in black and the white area is the burrow fill (scale bar = 0.5cm). Image B was obtained using simple image analysis.

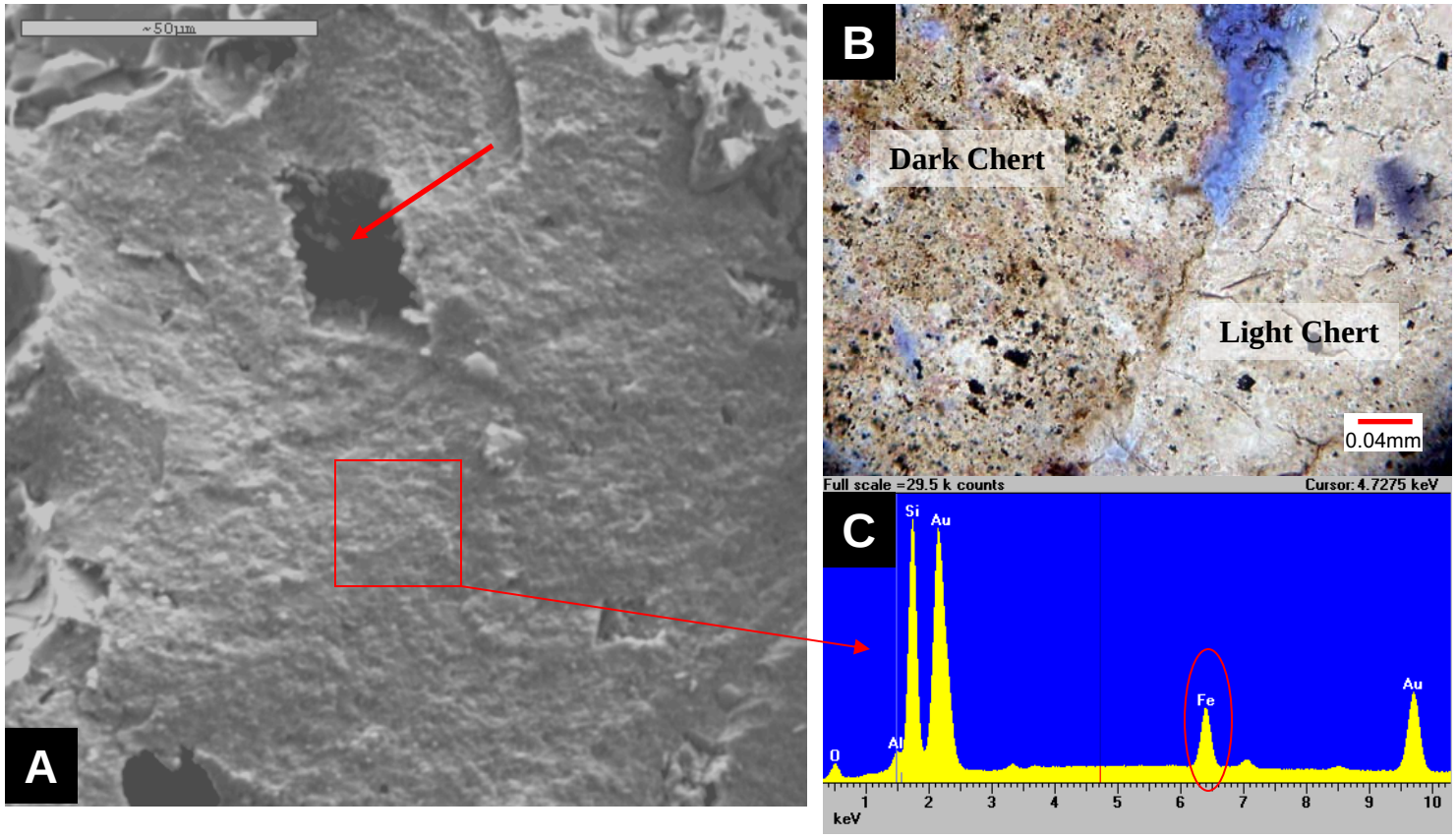

Figure 3.16 (A) Scanning electron photomicrograph of a dark-coloured chert grain. Note leached dolomite rhomb (arrow). Box indicates EDX scanned area. (B) Similar dark chert in thin section. (C) EDX analysis showing iron peak.

3.8 References

Brekke, H. G., 1995, Ichnology and sedimentology of the lower Cretaceous Bluesky formation, Sinclair field area, west central Alberta: Unpublished M. Sc. Thesis, University of Alberta, p165.

Clifton, H. E., and J. K. Thompson., 1978, *Macaronichnus segregatus* a feeding structure of shallow marine polychaetes: Journal of Sedimentary Petrology, v. 48, p. 1293-1302.

Dafoe, Lynn T., M. K. Gingras, and S. G. Pemberton., 2008, Analysis of mineral segregation in *Euzonus mucronata* burrow structures: one possible method used in the construction of ancient *Macaronichnus segregates*: Ichnos, 15:2, p.91-102.

Folk, R. L., 2002, Petrology of sedimentary rocks: Austin, Texas, Hemphill Publishing Company, p.127.

Gingras, M. K., B. MacMillan, B. J. Balcom, T. Saunders, and S. G. Pemberton, 2002, Using resonance imaging and petrographic techniques to understand the textural attributes and porosity distribution in *Macaronichnus*-burrowed sandstone: Journal of Sedimentary Research, v. 72, No. 4, p. 552-558.

Gingras, M. K., S. G. Pemberton, F. Henk, J. A. MacEachern, C. Mendoza, B. Rostron, R. O'Hare, and M. Spila, 2007, Applications of Ichnology to Fluid and Gas Production in Hydrocarbon Reservoirs, *in* J. A. MacEachern, K. L. Bann, M. K. Gingras, and S. G. Pemberton, eds., Applied Ichnology. Society of Economic Paleontologists and Mineralogists Short Course Notes 52, p. 127-141.

Landers, R. H., and R. E. Larese, and L. M. Bonnell, 2008, Toward more accurate quartz cement models: the importance of euhedral versus noneuhedral growth rates: American Association of Petroleum Geologists Bulletin, v.92, No. 11, pp. 1537-1563.

Larese, R. E., and D. L. Hall, 2003, Impact of interactive textural, compositional, and diagenetic controls on potential reservoir quality of low permeability sandstones (abs): AAPG Annual Convention Program, v.12, p. 98-99.

Mossop, G. D., and I. Shetsen, 1994, Geological Atlas of the Western Canada Sedimentary Basin. Canadian Society of Petroleum Geologists and Alberta Research Council: Chapter 19.

O'Connell, S., 1997, The recognition of a regional lowstand unconformity within the Bluesky Formation and its influence on production in the Sexsmith field, west central Alberta (abs.), CSPG-SEPM Joint Convention, Program with Abstracts, p. 210.

Pemberton, S. G., M. Spila, A. J. Pulham, T. Saunders, J. A. MacEachern, D. Robbins, and I. K. Sinclair, 2001, Ichnology and sedimentology of shallow to marginal marine systems: Geological Association of Canada, Short Course Notes, No.15, p. 353.

Pemberton, S. G. and M. K. Gingras, 2005, Classification and characterizations of biogenically enhanced permeability: American Association of Petroleum Geologists Bulletin, v. 89, p. 1493 – 1517.

Saunders, T.D.A. 1989, Trace fossils and sedimentology of a Later Cretaceous progradational barrier island sequence: Bear-paw-Horseshoe Canyon Formation transition, Dorothy, Alberta: Unpublished M. Sc. Thesis, University of Alberta, p.187.

Walsh, W. J. A., 1999, Sedimentology and sequence stratigraphy framework of the lower Cretaceous Bluesky Formation, Valhalla Area, west central Alberta: MSc thesis, Ottawa-Carleton Geoscience Centre and University of Ottawa, Ontario, 1999, p. 21-61.

Chapter 4: Conclusion

4.1 Introduction

This chapter summarizes the main findings of this thesis and includes a direction for further research in an attempt to better understand burrow associated reservoir quality and diagenetic reactions in marine sediments.

4.2 Research Findings in Chapter 2

Carbonate cement, silica cement, and authigenic clay are the most common pore occluding cements in marine sandstones and can severely reduce reservoir quality; however, secondary porosity due to dissolution of carbonate cement can leave an oversized pore system, increasing permeability and reservoir quality especially if the sand has been bioturbated previously as burrows can provide conduits within the sand than can increase permeability.

Recognition of early silica cement is important as pore systems that are cemented early with opaline cements were likely never charged with hydrocarbons. If these cemented pore systems are understood then adequate mapping will be required to avoid early silica cemented marine sandstones while exploring for hydrocarbons.

Equally as important is recognition of early pore-filling authigenic clay. These types of pore systems can misinterpreted as high pay zones

on wireline logging tools, but permeability is generally very low due to the microcrystalline structure of the clay.

Careful petrographic examination of fabric, texture, and mineral phase identification is essential to assessing reservoir quality in burrowed hydrocarbon bearing sediments. Detailed ichnological core work can lead to a better understanding of the depositional environments that contained trace fossil makers.

4.3 Research Findings in Chapter 3

The Bluesky Formation in the La Glace area in western Alberta is an upper shoreface deposit comprising fine to medium grained lithic sandstones with thin conglomeratic lag deposits and fine grained carbonate cemented storm beds. Within the lithic sand is a medium grained litharenite interval heavily bioturbated with *Macaronichnus segregatus*. This bioturbated zone is indicative of high-energy shoreface deposits, shows an elevated preserved permeability than in the surrounding sediment, and is the target of hydrocarbon exploitation.

Petrographic techniques have aided in understanding the effects *Macaronichnus segregatus* has on reservoir quality in these upper shoreface sediments. Utilization of thin sections and scanning electron microscopy has lead to the interpretation that the tracemaker of *Macaronichnus segregatus* avoided iron-rich detrital fragments while exploiting the sediment for food. This grain avoidance lead to a re-sorting

of the sand that shed the dark coloured rock fragments to outline the burrow while light coloured competent grains were ingested and became the burrow fill. The light coloured burrow-fill contains a high chert to quartz ratio. Primary reservoir quality can be preserved in the presence of chert as pore-occluding quartz overgrowths do no form on chert fragments as they do on monocrystalline quartz, thus leaving open, well connected primary pores and hence elevated permeability. Chert fragments are resistant to the effects of mechanical compaction and are not easily squeezed into adjacent pore space as are ductile rock fragments.

4.4 Future Research

Petrographic techniques have proved to be a valid technique in understanding burrowed-associated pore systems in marine sandstones. It is a necessary first step in reservoir evaluation, but it often overlooked by more quantitative methods such as wireline log evaluation and engineering numerical models. While extremely useful, these techniques fail to recognize textural and fabric characteristics that can be affected by burrowing fauna that have an impact on reservoir quality. In the future, a more multidisciplinary approach is required. Petrologists, petrophysicists, play geologists, ichnologists, and engineers need to work together to understand the cause and effect of burrow-associated hetrogeneities. These heterogeneities present notable complications on the completion and production optimization for reservoir development.

Petrographic work alone does present some limitations. Diagenetic reactions can be complex. This is especially true in reservoir sandstones that have undergone deep burial and subsequent uplift. Many eogenetic mineral phases can become overprinted by telogenetic mineral alterations. These alterations skew eogenetic fabric and texture leading to a possible misinterpretation of the diagenetic history of the reservoir.

Stable isotope analysis, bulk chemistry analysis, and cathodoluminescence microscopy can aid with better interpretations of mineral paragenesis. These techniques are often expensive and consume time that may not fit the financial model of hydrocarbon play generation, but do provide excellent data when there is question about mineral phase paragenesis.

Ichnological interpretation provides important paleoenvironmental data that can aid in mapping burrow-associated reservoir quality. Understanding the behaviour of burrowing fauna can lead to better hydrocarbon play mapping as the geologist can lean away from areas where extensive burrow-mediated cementation has occurred and attempt to better map areas where cement dissolution has taken place. This may be especially important for emerging tight gas and shale plays where permeability streaks in bioturbated sediment are abundant.

Legend

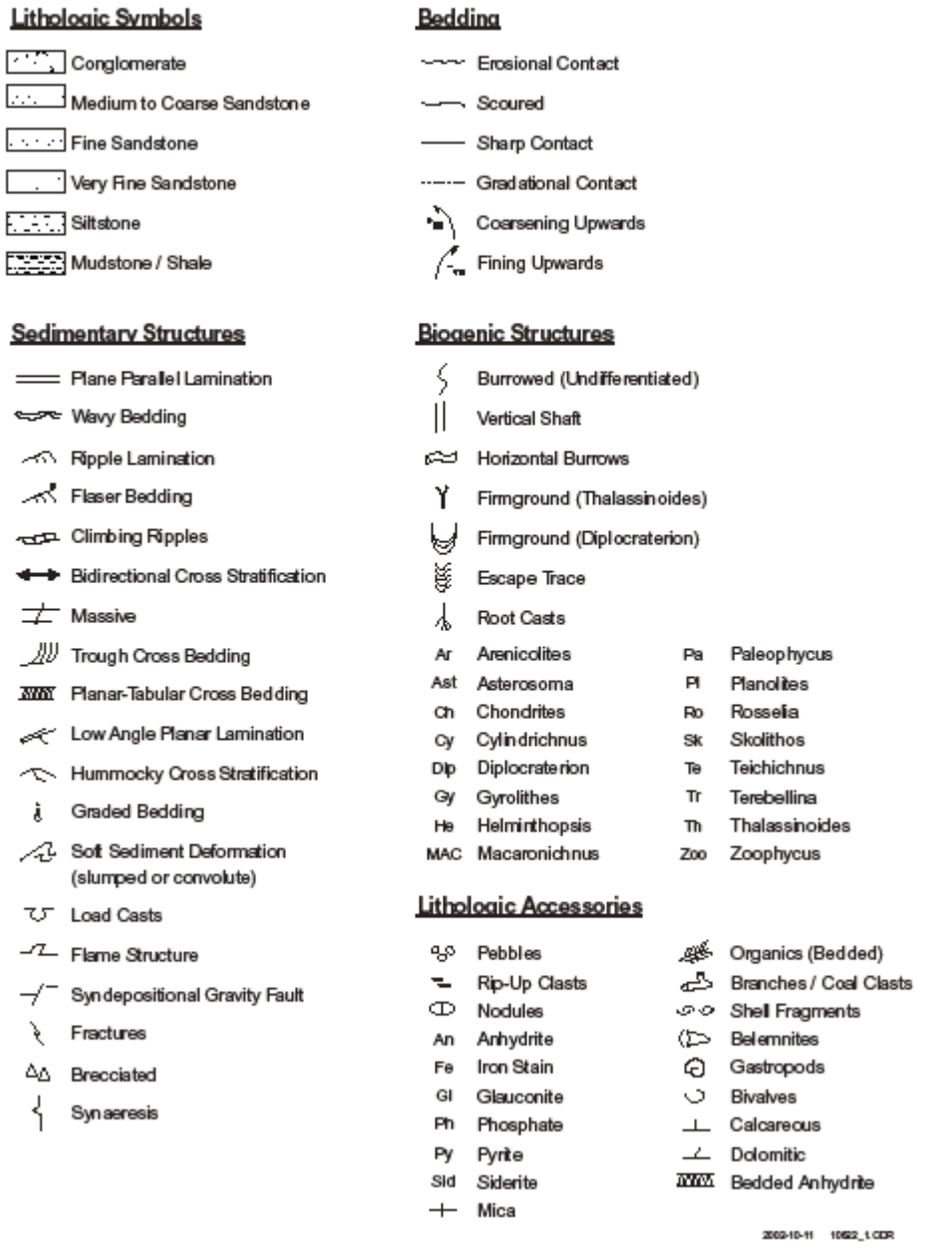

Appendix 1. Core descriptions for Chapter 3.

Well Name: Enron et al La Glace 06-04-074-07W6

Formation: Bluesky

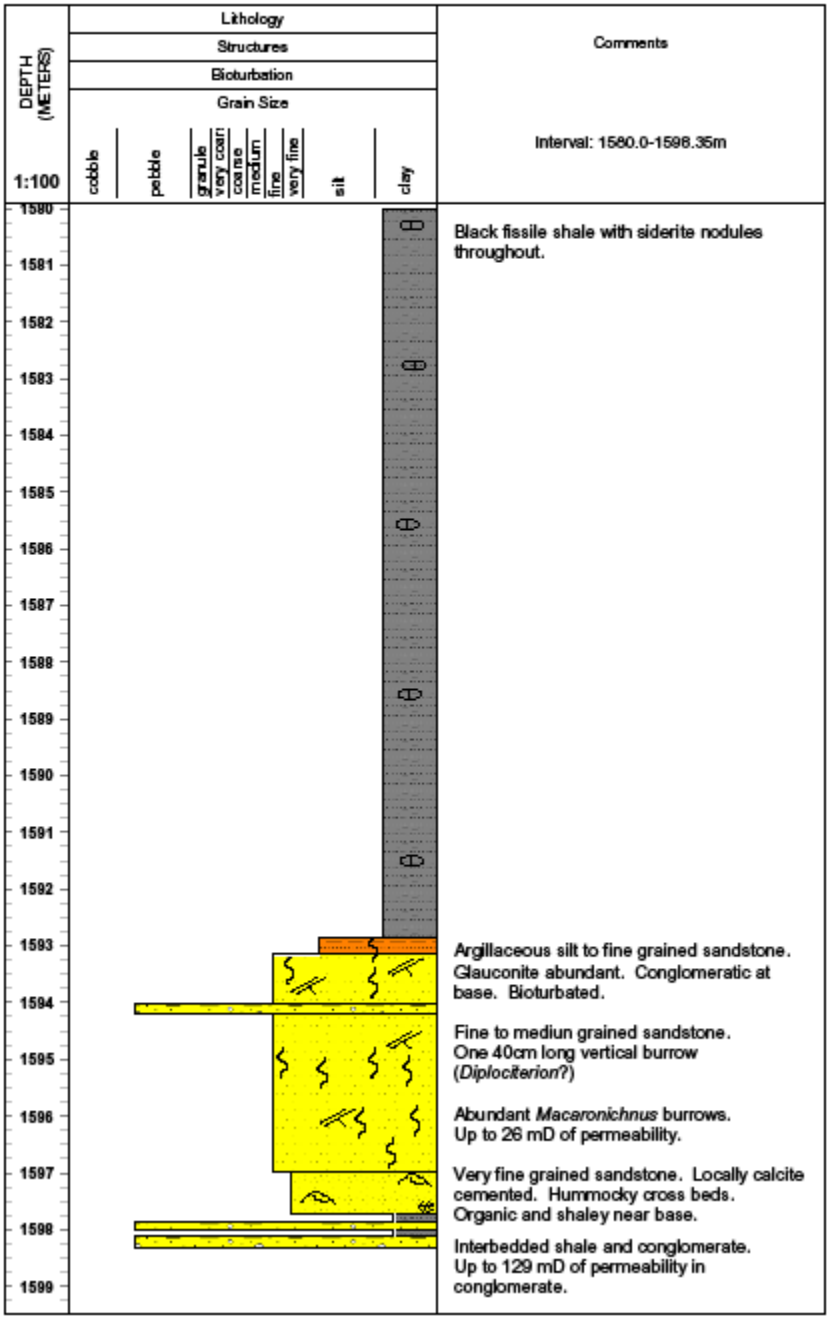

Appendix 1. Core descriptions for Chapter 3.

Well Name: Enron et al La Glace 14-08-074-07W6

Formation: Bluesky

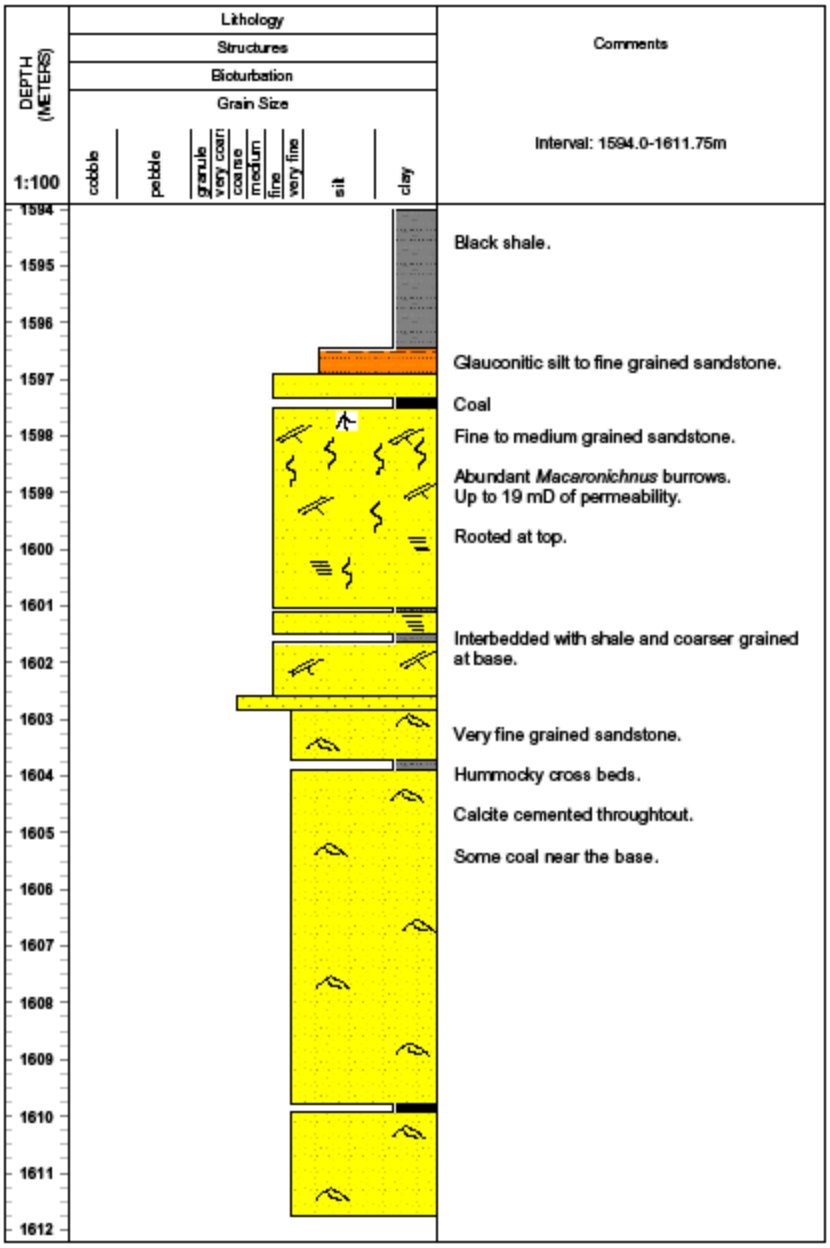

Appendix 1. Core descriptions for Chapter 3.

Well Name: Enron et al Sexsmith 16-10-074-07W6

Formation: Bluesky

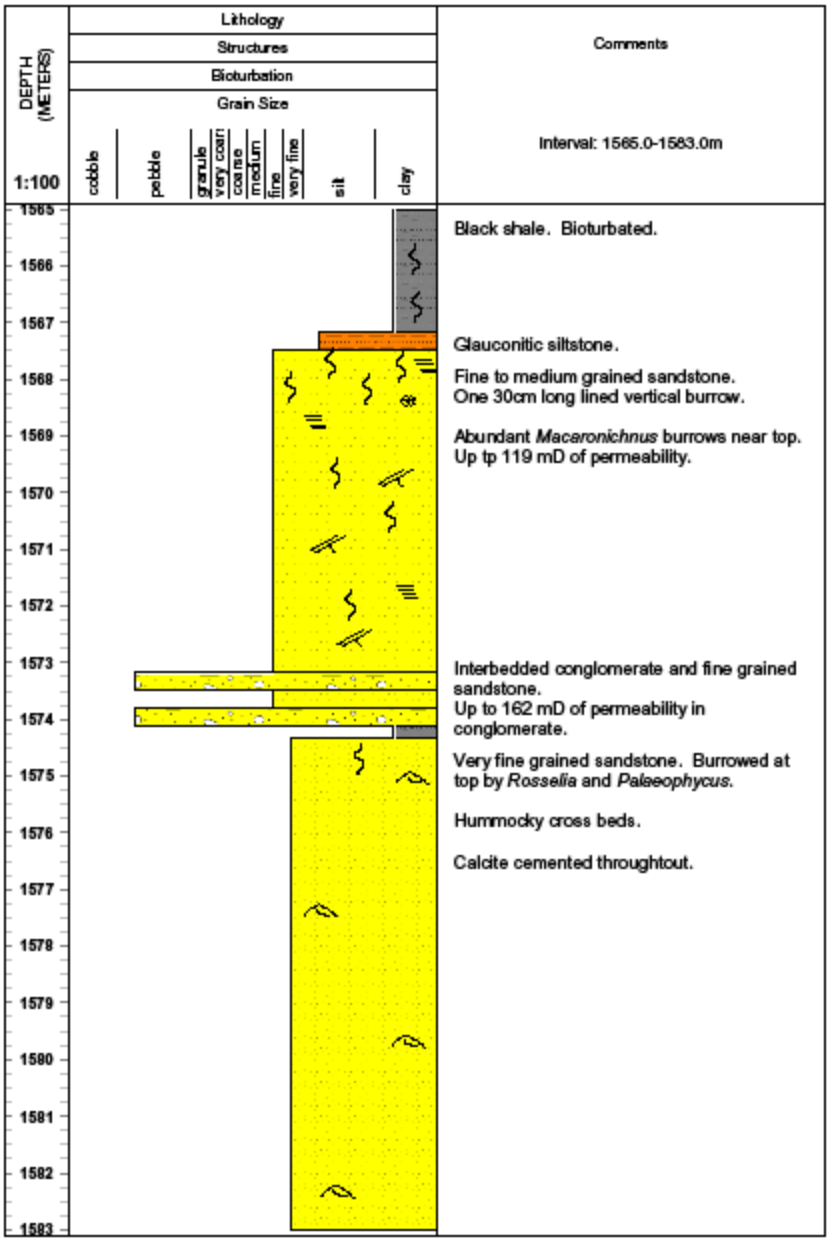

Appendix 1. Core descriptions for Chapter 3.

Well Name: Enron et al La Glace 11-18-074-07W6

Formation: Bluesky

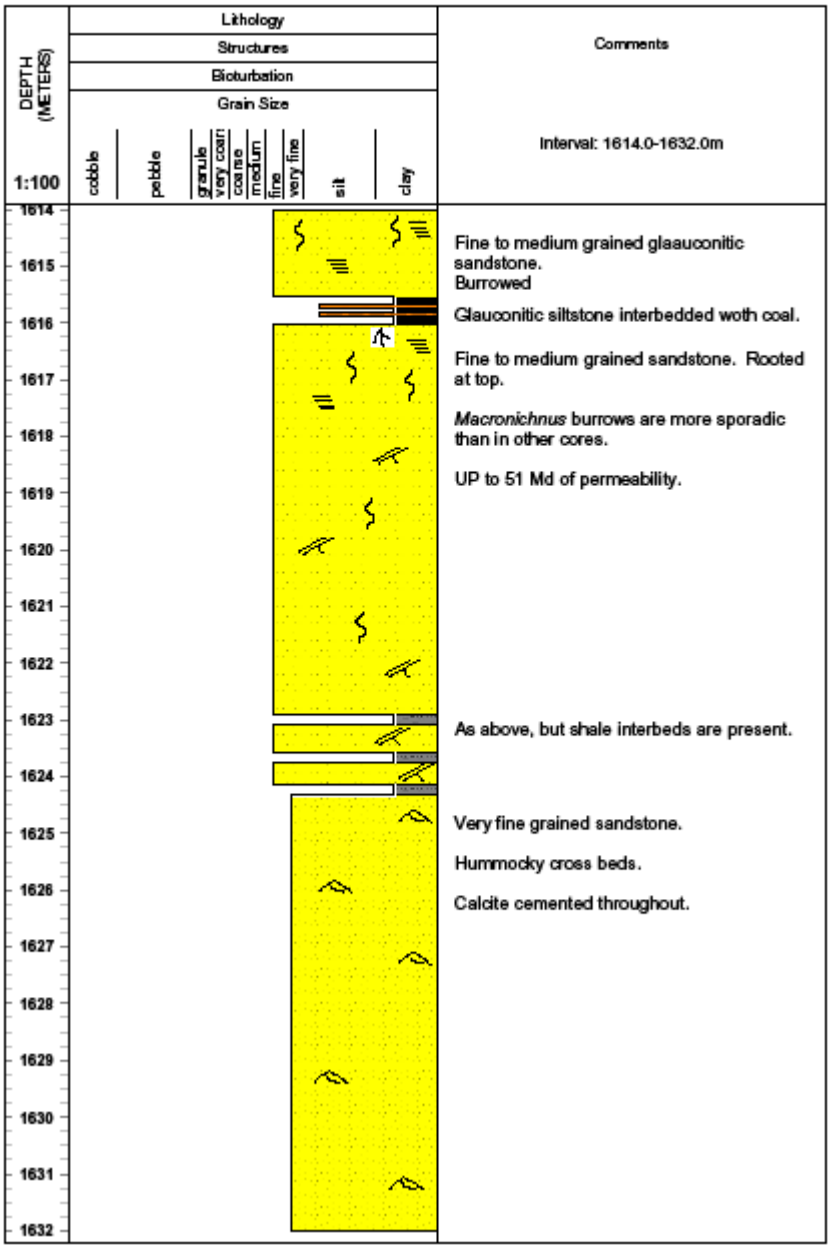

Appendix 1. Core descriptions for Chapter 3.

Well Name: Encor et al Sexsmith 14-21-074-07W6

Formation: Bluesky

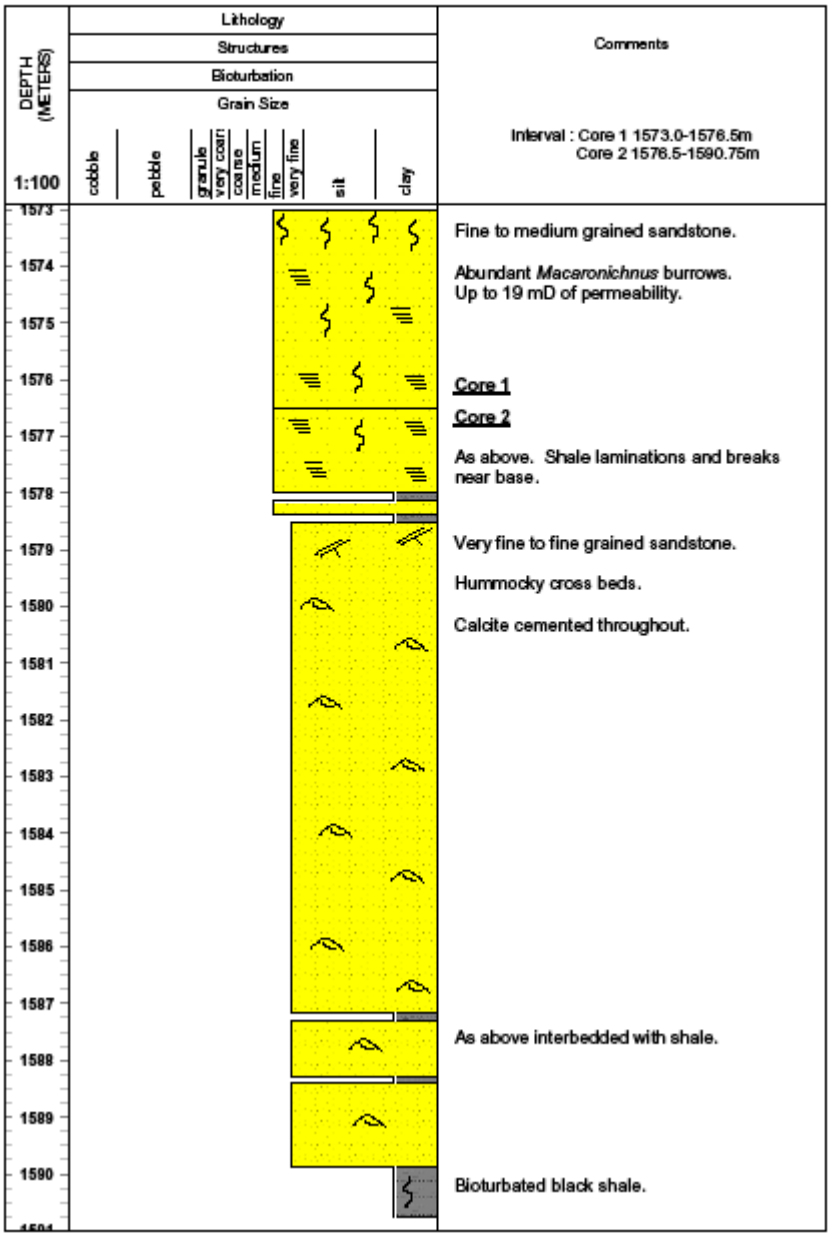

Appendix 1. Core descriptions for Chapter 3.

Well Name: Talisman et al La Glace 06-24-074-07W6

Formation: Bluesky

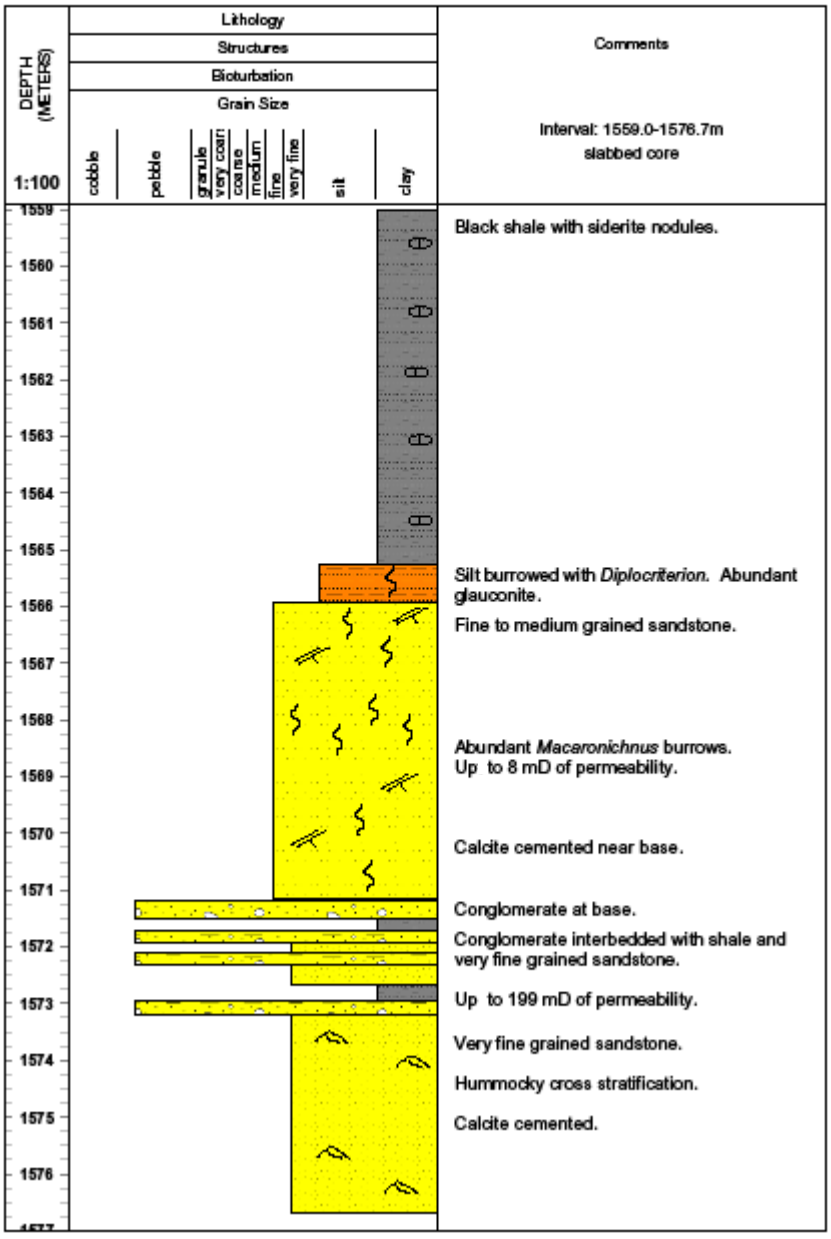

Appendix 1. Core descriptions for Chapter 3.